The Structure and Evolution of Cold Surges East of the Rocky Mountains

BRIAN A. COLLE AND CLIFFORD F. MASS

Department of Atmospheric Sciences, University of Washington, Seattle, Washington

(Manuscript received 3 May 1994, in final form 10 January 1995)

ABSTRACT

Northerly surges of cold air often move southward along the eastern side of the Rockies from southern Canada into Mexico. The strongest surges, which generally develop in midwinter, are associated with temperature decreases and pressure rises of 20°–30°C and 15–30 mb, respectively, within 24 h. Surges are usually accompanied by a meridionally elongated pressure ridge and strong low-level ageostrophic winds that parallel the terrain. The width of the pressure ridging is approximately 1000 km over the southern plains but decreases to only a few hundred kilometers when the surge enters Mexico.

This paper provides a detailed description of a northerly surge to the east of the Rocky Mountains that occurred on 12–14 November 1986. Using both observational and model data, the structural evolution of the surge is analyzed; in addition, the dynamics of the event is explored by diagnosing the momentum, thermodynamic energy, and vorticity equations. To determine the typical synoptic-scale evolution of these cold surges, a composite study is also presented. It is concluded that these cold surges result primarily from the interaction of the evolving synoptic-scale flow with the Rocky Mountains and the sloping topography of the Great Plains, and not from the generation of rotationally trapped waves such as Kelvin, shelf, and topographic Rossby waves. When an upper-level short-wave trough moves southeastward out of western Canada, northerlies, high pressure, and cold air spread southward into the northern plains at low levels. Lee troughing occurs to the east of the central and southern Rockies and, in concert with the ridging to the north, establishes an along-barrier pressure gradient that forces ageostrophic northerly flow and the meridional advection of cold air. Blocked upslope flow at the forward portion of the surge leads to large-scale damming. As the surge enters Mexico, where the topography becomes steeper and the large-scale slope is lost, the width of the damming is greatly reduced. Consistent with damming, momentum diagnostics over both the Great Plains and coastal Mexico indicate that an antitriptic balance exists parallel to the mountains, whereas a geostrophic balance exists normal to the barrier.

1. Introduction

a. Background

Shallow surges of cold air often propagate parallel to major mountain ranges such as the Himalayas, Rockies, Appalachians, Alps, and the Great Australian Dividing Range. On the lee side of the Rocky Mountains such surges are common from late fall through early spring and are often accompanied by strong lower-tropospheric northerly winds exceeding 20 m s^{-1}, as well as rapid decreases in temperature and sharp rises in pressure, frequently reaching 20°–30°C and 15–30 mb, respectively, within 24 h. As noted by Bluestein (1993), a rapid increase in surface northerlies sometimes leads a sharp decline in temperature; thus, in this paper, the leading edge of the surge is defined by a transition to strong northerly flow at the surface. Cold surges are usually accompanied by surface pressure ridges that often have widths (normal to the Rockies) of over 1000 km across the sloping terrain of the Great Plains. These surges can propagate southward from western Canada into Mexico in two to three days even with primarily zonal mid- and upper-tropospheric flow. Over coastal Mexico, the width of the ridging decreases from approximately 1000 to 2000 km to 300 km. Occasionally, surges propagate into southern Mexico and cross the Isthmus of Tehuantepec, producing strong winds ("tehuantepecers") over the coastal Pacific Ocean.

Since cold surges move with the topography to the right (left) in the Northern (Southern) Hemisphere, some investigators (Leathers 1986; Hsu 1987; Tilley 1990) have discussed their dynamics in terms of rotationally trapped waves, such as Kelvin, shelf, and topographic Rossby waves (sometimes referred to as edge waves); in addition, the northerly surges resemble other rotationally trapped features such as topographically trapped gravity currents (Baines 1980) and cold-air damming (Bell and Bosart 1988). In the next section, previous theoretical and observational studies of such terrain-bound features are reviewed.

Corresponding author address: Brian A. Colle, Dept. of Atmospheric Sciences, Box 351640, University of Washington, Seattle, WA 98195-1640.
E-mail: colle@atmos.washington.edu

b. Rotationally trapped atmospheric phenomena

1) KELVIN WAVES

When a stable fluid is bounded on the right by a steep barrier in the Northern Hemisphere (left in the Southern Hemisphere), the flow can become trapped rotationally by the Coriolis force and Kelvin waves may result (Gill 1982). Kelvin waves have no wind component perpendicular to the barrier. If one neglects nonlinear terms, geostrophic balance exists in the cross-barrier direction, and the local acceleration and pressure gradient are balanced in the along-barrier direction. Linear Kelvin waves are nondispersive; have a phase speed for the stratified case equal to $(g^*H)^{1/2}$, where g^* is reduced gravity $(g\Delta\rho/\rho)$ and H is the undisturbed depth; and possess a length scale perpendicular to the barrier of a Rossby radius of deformation, $(g^*H)^{1/2}f^{-1}$. Keeping the nonlinear terms can lead to solitary Kelvin waves if the dispersive effects balance the nonlinearities (Reason and Steyn 1992). The phase speed of a solitary wave is equal to $[g^*H(1 + \alpha)]^{1/2}$, where α is the amplitude of the wave.

It has been suggested that various along-barrier surge phenomena around the world have Kelvin wave characteristics. Gill (1977), Anh and Gill (1981), Bannon (1981), and Reason and Jury (1990) noted that South African coastal lows have a similar structural evolution to internal Kelvin waves, with the steep African coastal plateau and a strong low-level inversion trapping these features both horizontally and vertically. Dorman (1985) suggested that coastal southerlies along the United States west coast have horizontal widths and phase speeds similar to those of Kelvin waves. However, Mass and Albright (1987) showed that such trapped southerly flow could be better explained as a topographically trapped density current or flow down the synoptic-scale along-barrier pressure gradient. Sumi and Toyota (1988), Sumi (1985), and Tilley (1990) showed that the leading edge of southward-moving surges along the Himalayas had phase speeds and Rossby radii similar to those expected from Kelvin wave theory. Webster and Fritsch (1985) and Tilley (1990) suggested that surges moving southward to the east of the Rocky Mountains have Kelvin wave characteristics because low-level flow was parallel to the terrain and the surge propagation speed ($\sim$25–35 m s^{-1}) was apparently much faster than the advective velocity.

2) TOPOGRAPHICALLY TRAPPED GRAVITY CURRENTS

Closely related to Kelvin waves are topographically trapped density currents. Like a Kelvin wave, a trapped density current has a horizontal scale on the order of a Rossby radius, there is no wind component normal to the barrier, geostrophic balance exists in the cross-barrier direction, and the acceleration and pressure gradient terms are balanced in the along-barrier direction for inviscid flow (Baines 1980). The primary difference between Kelvin waves and trapped gravity currents is that the former involves wavelike transverse displacements of a stably stratified fluid, whereas in the latter, a cooler, more dense fluid replaces a warmer, less dense one.

Baines (1980) suggested that "southerly busters," coastal surges that propagate along the southeastern coast of Australia, are topographically trapped gravity currents. Occurring primarily in the spring and summer, busters are usually accompanied by mesoscale pressure ridging in the coastal zone, a rapid wind shift, gusty southerly winds, and a rapid temperature decrease (Wilson and Stern 1985; Colquhoun et al. 1985; Coulman et al. 1985). Both Holland and Leslie (1986) and Tilley (1990) suggested that the strong mesoscale terrain-parallel winds are a result of Kelvin waves. However, McBride and McInnes (1993) argued that the buster seems more of a "current" than a "wave" because the mass field is highly advective.

Trapped density currents have been noted at other locations. Mass and Albright (1987) interpreted an alongshore surge of cool marine air along the west coast of North America as a topographically trapped gravity current. Hoinka and Volkert (1992) suggested that some of the fronts analyzed north of the Alps in the German Front Experiment of 1987 had trapped density current characteristics, such as sudden pressure jumps and the presence of roll clouds.

3) AGEOSTROPHIC DOWNGRADIENT FLOW AND COLD-AIR DAMMING

Overland (1984), Mass and Albright (1987), and Overland and Bond (1993) have noted that ageostrophic downgradient flow can be forced by an along-barrier pressure gradient imposed by the synoptic-scale pressure field. Using scale analysis, Overland and Bond (1993) showed that when l/L (cross-barrier length scale/along-barrier length scale) is small and the Rossby number $R_l = V/fl$ (where V is the magnitude of the along-barrier flow) is approximately equal to or greater than one, the winds are primarily terrain-parallel, with the along-barrier pressure gradient primarily balancing the along-barrier acceleration and friction, and the mass field adjusting so that the pressure gradient normal to the terrain balances the Coriolis force associated with the terrain-parallel winds. Overland and Bond (1993) noted that for steep topography, these balances extend from the barrier approximately a Rossby radius of deformation, $l_R = Nh_m/f$ (where N is the buoyancy frequency and h_m is the height of the ridge).

There are several examples of such dynamics. Nakamura and Murakami (1983) noted that for cold surge events east of the Himalayas, the establishment of an along-barrier pressure gradient induced by a strong anticyclone to the north and a lee cyclone to the south

leads to strong ageostrophic northerlies over the sloping terrain. Mass and Albright (1987) showed that when the synoptic-scale pattern establishes an along-barrier pressure gradient along the coastal topography of California under stable summertime conditions, the winds flow ageostrophically downgradient within approximately a Rossby radius of the terrain (few hundred kilometers). Lackmann and Overland (1989) noted that when the isobars are orientated normal to the Shelikof Strait in Alaska, downgradient gap flow occurs. Overland and Bond (1993) showed that when a strong cold front moved inland across western British Columbia, ageostrophic downgradient flow developed offshore within a few hundred kilometers of the steep coastal terrain.

Cold-air damming, and Appalachian cold-air damming in particular, can also be explained using these dynamics (Bell and Bosart 1988). Baker (1970), Kieser (1987), and Bell and Bosart (1988) showed that Appalachian damming is most frequent during winter and early spring when high pressure over the New England states and developing low pressure over the southeast United States leads to a strong along-barrier pressure gradient. With such a pressure gradient, ageostrophic downgradient flow approximately parallel to the Appalachians develops and advects cold air southward along the eastern slopes of the barrier. The Coriolis force acts on the northerly flow producing an upslope component that pushes the cold air against and up the terrain. The synoptic-scale flow may also have a component normal to the mountain, which can also contribute to advecting the cold air up the barrier. Because the Froude numbers[1] are less than unity in most cold-air damming structures (Bell and Bosart 1988), the cold air is blocked (or dammed) by the terrain and a "dome" of cold air develops adjacent to the barrier (Forbes 1987). As a result, there is ridging in the lower-tropospheric pressure field along the eastern slopes of the barrier. After a short period of adjustment, a steady-state balance occurs in which the Coriolis force associated with the along-barrier flow is in approximate geostrophic balance with the cross-barrier pressure gradient force caused by mass accumulation next to the mountain. In the along-barrier direction, an antitriptic balance develops between the along-barrier component of the synoptic-scale pressure gradient force and friction.

Cold-air damming has also been suggested at other locations. Dunn (1987) described mesoscale damming along the Colorado Front Range, while Mass and Albright (1985) have documented damming east of the Cascade Mountains.

4) TOPOGRAPHIC ROSSBY AND SHELF WAVES

In contrast to the steep orography associated with mesoscale Kelvin waves and trapped gravity currents, sloping topography can cause trapped phenomena on the synoptic scale. These larger, trapped features are maintained by fluid motion conserving its potential vorticity on a sloping surface (the equivalent beta effect). Newton (1956) used potential vorticity conservation to argue that vortex stretching associated with downslope winds on the southern flank of Rocky Mountain lee cyclones result in their southward movement. This theory was later expanded such that if the slope is small, so that the quasigeostrophic system is valid, the fluid motions up and down the slope result in the generation of low-frequency (less than f) bottom-trapped features called topographic Rossby waves (Rhines 1970). When the slope increases, the winds perpendicular to the barrier can no longer remain quasigeostrophic and shelf waves can occur (Pedlosky 1987).

Because both topographic Rossby and shelf waves share the same basic physics (the conservation of potential vorticity), they essentially have the same structure and propagation characteristics. Both propagate with higher terrain to the right (left) in the Northern (Southern) Hemisphere. The primary difference between topographic Rossby and shelf waves is that the latter is characterized by predominantly terrain-parallel flow, whereas topographic Rossby waves have more of an upslope component (Pedlosky 1987). Gill (1982) noted that unlike Kelvin modes, shelf and topographic Rossby waves are generally dispersive (the longest shelf waves can be nondispersive) and have larger horizontal scales (roughly scale of the slope) and slower phase speeds than Kelvin modes.

Because trapped cold surges adjacent to the Tibetan Plateau and Rocky Mountains exhibit larger scales and slower phase speeds than Kelvin waves, Hsu and Wallace (1985) suggested that they are trapped topographic Rossby waves. Hsu (1987) noted that both positive and negative anomalies propagate southward along the barrier and have a scale comparable to that of the terrain. Therefore, he concluded that trapped topographic Rossby waves were evident. Tilley (1990) suggested that larger trapped modes (e.g., topographic Rossby waves and shelf waves) exist within the larger-scale ridging of cold surges and are generated by upslope motions within the cold dome. Tilley hypothesized that the onset of these larger-scale trapped waves corresponds to a secondary temperature gradient and the strengthening of the terrain-parallel winds behind the initial surge.

c. Motivation and objectives

Although there has been considerable discussion of southward-propagating trapped surges along the eastern slopes of the Rockies, there has been relatively little

[1] The Froude number $U(h_m N)^{-1}$ is a measure of the kinetic energy of the upslope flow to the potential energy necessary to lift the fluid over the barrier. Here, U is the upslope wind component.

detailed examination of the structural evolution and dynamics of specific cases. To address this deficiency, this paper provides a detailed description of the evolution, structure, and dynamics of the surge event of 12–14 November 1986, using both observations and model simulations. Various mechanisms are evaluated using diagnostics involving the thermodynamic, vorticity, and momentum equations. In addition, to determine the role of the Gulf of Mexico during these surges, a sensitivity study was completed in which the gulf was converted into a land. Before presenting this case study, the composite large-scale evolution of these surges is described.

2. Composite study

To determine the typical large-scale evolution associated with cold surges east of the Rocky Mountains, a composite study of 39 events was created. Selected events had to meet two criteria simultaneously. First, since cold surges move southward over the Great Plains and are usually associated with anticyclones with central pressures greater than 1035 mb, the first requirement was that the sea level pressure over central Nebraska had to be greater than or equal to 1035 mb. Second, because the leading edge of a cold surge is usually associated with a large pressure rise over the southern plains, the 12-h isallobaric rise in north-central Texas had to be equal to or greater than 10 mb. A total of 39 events (listed in Table 1) met these criteria for the period 1965–89. These surges are generally wintertime phenomena, with December and January having the greatest number of occurrences and no events occurring between May and October. For each event, the time that the above conditions are first met is defined as the zero hour (0 h).

Fields for the composites were taken from the National Meteorological Center (NMC) Grid Point Data Set on compact disc (Mass et al. 1987). This dataset is based on the NMC's operational Northern Hemispheric analyses, which have a resolution of 380 km and are available at 0000 and 1200 UTC. Composites were created by averaging the NMC analyses relative to the zero hour. Deviations of the composites from climatology were also constructed. Climatology fields (Fig. 1) were made by calculating weighted monthly means, in which the weighting is dependent on the number of events that occur during each month. A two-tailed Student's t-test (Panofsky and Brier 1968) was used to determine the statistical significance of the deviations from climatology.

Figure 2 shows the composite fields of 500-mb heights, deviations of the composite heights from climatology, and the statistical significance of the deviations, from 24 h before to 24 h after the 0 h. During this period, west-northwest flow over the Rockies at the initial time becomes more northwesterly as a short-wave trough moves southward out of Canada and deepens the long-wave trough over the eastern United States. The 700-mb height composites (not shown) follow a similar evolution.

TABLE 1. Surge events used in the composite.

1200 UTC 16 Jan 1966	0000 UTC 9 Feb 1979
0000 UTC 23 Dec 1966	0000 UTC 16 Feb 1979
1200 UTC 15 Mar 1967	0000 UTC 17 Dec 1979
0000 UTC 7 Jan 1968	1200 UTC 31 Jan 1980
1200 UTC 12 Jan 1968	1200 UTC 8 Feb 1980
1200 UTC 13 Feb 1968	1200 UTC 1 Mar 1980
1200 UTC 7 Dec 1968	1200 UTC 19 Dec 1980
0000 UTC 6 Jan 1970	1200 UTC 24 Dec 1980
0000 UTC 23 Nov 1970	1200 UTC 14 Apr 1981
1200 UTC 15 Dec 1972	0000 UTC 11 Jan 1982
0000 UTC 28 Jan 1973	1200 UTC 16 Jan 1982
1200 UTC 8 Feb 1973	0000 UTC 25 Dec 1983
1200 UTC 19 Dec 1973	1200 UTC 18 Jan 1984
1200 UTC 24 Feb 1974	1200 UTC 20 Jan 1985
0000 UTC 18 Dec 1975	1200 UTC 7 Jan 1986
1200 UTC 7 Jan 1976	0000 UTC 13 Nov 1986
1200 UTC 18 Jan 1977	1200 UTC 11 Feb 1988
1200 UTC 9 Dec 1977	1200 UTC 15 Dec 1988
1200 UTC 1 Jan 1978	0000 UTC 5 Mar 1989
1200 UTC 8 Jan 1978	

Composite fields of sea level pressure, deviations of the composites from climatology, and statistical significance of the deviations are shown in Fig. 3. At −48 h, strong high pressure, significant to the 99% level, is over the Yukon Territory. A negative anomaly exists over the northern American Rockies, the eastern portion of which is associated with weak lee troughing, with the remainder reflecting the approaching short-wave trough. By −24 h, the along-barrier pressure gradient increases dramatically as lee troughing becomes stronger and high pressure moves southward out of Canada.[2] Both of these features are significant at the 99% level. Between −24 h and 0 h, the lee trough moves southward and dissipates, while high pressure thrusts southward into Mexico. Between +24 and +48 h, one area of positive deviations moves eastward with the upper-level synoptic forcing, while another hangs back over the southern plains and Mexico.

Figure 4 presents the evolution of the thermal field at 850 mb. At −48 h, a strong temperature gradient exists near the United States–Canada border, especially over western Canada. Although weak at −48 h, the warm tongue on the lee side of the southern Rockies strengthens and becomes statistically significant by −24 h. By 0 h, a tongue of cold air extends southward

[2] Most of the 39 composite cases had this lee trough develop as a result of strong cross-barrier flow. However, a few cases had a short-wave trough moving across the Colorado Rockies or a weak cutoff low drifting eastward from the southwestern states toward the southern plains.

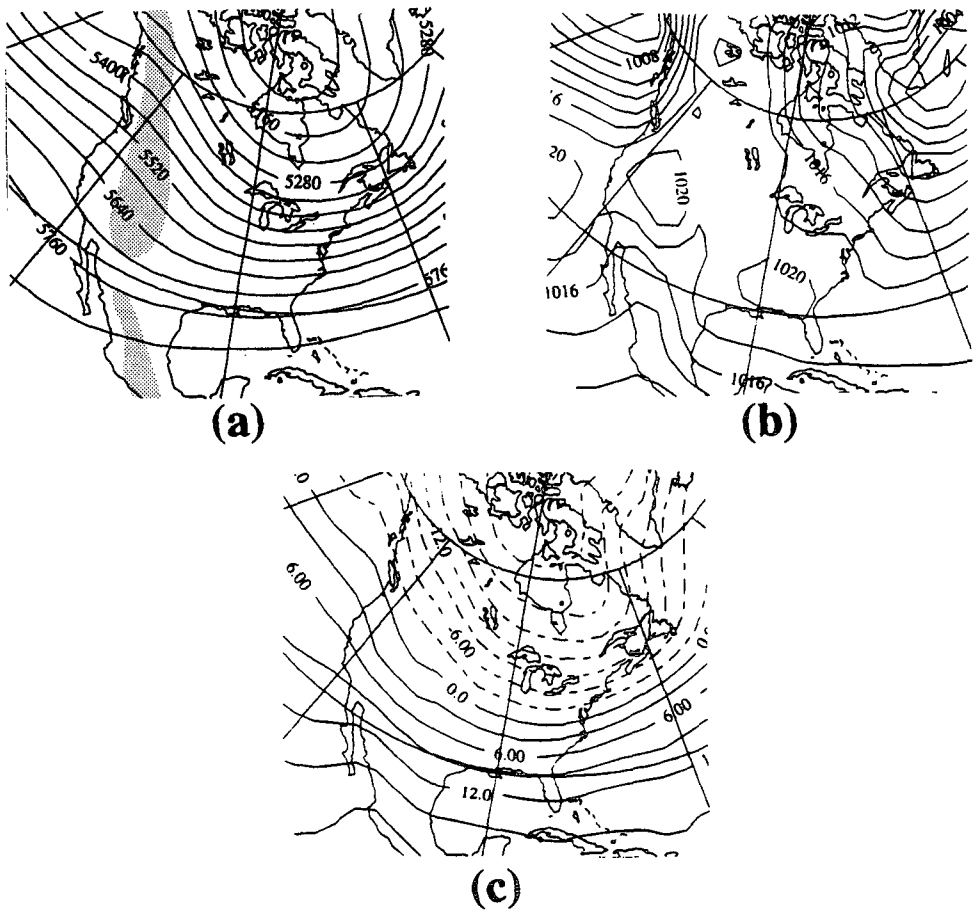

FIG. 1. Climatological fields of (a) 500-mb height, (b) sea level pressure, and (c) 850-mb temperature. Heights are in meters and pressures are in millibars. The shaded region in (a) indicates terrain elevation greater than 1500 m.

into Mexico, and the warm anomaly has disappeared. At +24 and +48 h, temperature and its deviation from climatology evince a two-lobe structure, with one portion moving eastward to the Ohio Valley with the synoptic-scale forcing and the other remaining over Texas and Mexico.

3. Observational overview of the 12–14 November 1986 cold surge

a. Horizontal structure

This section provides a brief observational overview of the strong northerly surge that occurred along the eastern side of the Rockies between 0000 UTC 12 November 1986 and 1200 UTC 14 November 1986.

At 0000 UTC 12 November 1986, an anticyclone was located over eastern British Columbia and western Alberta, and the leading edge of the surge stretched from central Wyoming northeastward into southeastern North Dakota (Fig. 5a).[3] At the surface, a weak low center was located along the eastern slopes of the Colorado Rockies and extended southward into New Mexico and Texas, while at 850 mb a trough extended northward from New Mexico into central Canada (Fig. 5b). Another surge had moved southward to the east of the Rockies two days earlier, leaving a tongue of weak high pressure from the Midwest into Texas. At 500 mb, there was northwesterly flow over the western United States, a long-wave trough covered the central United States, and a short-wave trough was over Montana (Fig. 5c).

By 0600 UTC 12 November, the weak low center, coincident with downslope flow below 700 mb, had deepened 2 mb and moved southward to the Oklahoma panhandle (not shown). The leading edge of the surge was located over northeastern Colorado and southern

[3] The leading edge of the surge, denoted by the dark solid line in Fig. 5a and in subsequent figures, is defined as the leading edge of the transition to strong northerly flow at the surface.

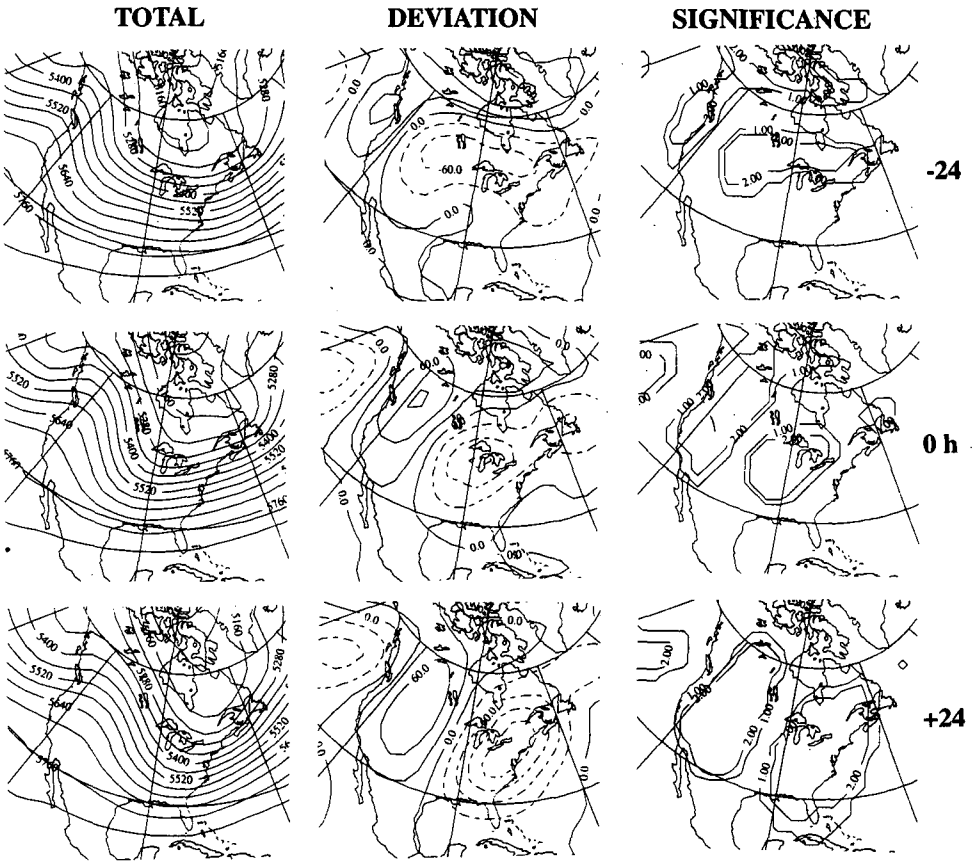

FIG. 2. Geopotential heights and height deviations from climatology at 500 mb, and statistical significance of the deviations for the composite event. The contour intervals are 60 m for the total composites and 30 m for the deviations. Significance levels of 95% and 99% are indicated by 1.00 and 2.00, respectively.

Nebraska at that time. Subsequently, the low weakened and moved southward, leaving only a weak trough over western Texas at 1200 UTC 12 November (Fig. 6a). At the surface, the leading edge of the surge was over the Texas panhandle and central Oklahoma, and at 850 mb a tongue of cold air extended southward along the eastern side of the Rockies (Fig. 6b). At 500 mb (Fig. 6c), the short-wave trough over the northern plains had moved southeastward, with a ridge (not completely shown) over the West Coast.

During the next 12 h the leading edge of the surge over both the sloping terrain of Texas and the more level terrain to the east moved at about 15 m s^{-1}, which was close to the advective speed. By 0000 UTC 13 November, the surge had reached the Mexican border, and a surface anticyclone extended over the sloping terrain of the southern plains (Fig. 7a).[4] Winds over the western plains were predominantly terrain parallel, except for an upslope wind component along the leading edge of the surge. At 850 mb, a tongue of cold air extended from Kansas into southwestern Texas (Fig. 7b). At 500 mb, the flow was from the west-northwest over the surge region (Fig. 7c).

At 0000 UTC 14 November (Fig. 8a), a tongue of high pressure extending southwestward from the main anticyclone over Illinois narrowed to only a few hundred kilometers along coastal Mexico. The pressure ridging over Texas and coastal Mexico was mainly the result of cold air being banked up against the sloping terrain, as seen in the 850-mb wedge-shaped cold tongue along the Rockies and the Mexican coast (Fig. 8b). At this time, the 500-mb trough was approaching the East Coast, and another short-wave trough was moving southeastward across the Dakotas (Fig. 8c). By 1200 UTC 14 November (not shown), the tongue of high pressure over the southern plains weakened as the main high pressure center drifted eastward toward the Appalachians.

b. *Vertical structure*

To demonstrate the effects of the northerly surge on vertical structure, Fig. 9 shows the soundings at Rapid

[4] Even though strong northerly winds extended along the Texas gulf coast (Fig. 7a), the leading edge of the surge was placed farther to the north given the 850-mb winds (Fig. 7b).

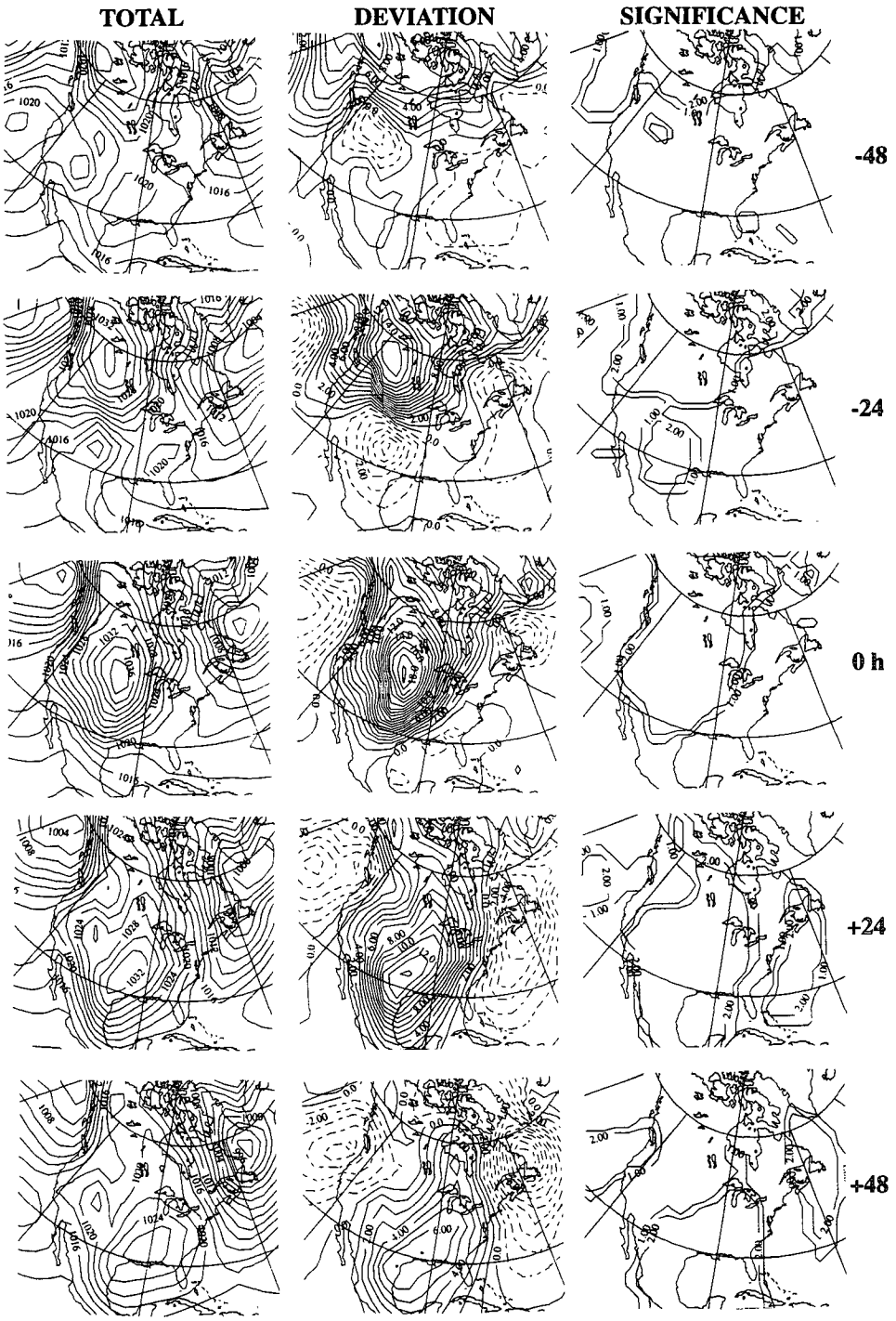

FIG. 3. Sea level pressure, deviations from climatology, and statistical significance of the deviations for the composite event. The contour intervals are 2 mb for the total composites and 1 mb for the deviations. Significance levels of 95% and 99% are indicated by 1.00 and 2.00, respectively.

City, South Dakota (RAP); Dodge City, Kansas (DDC); Midland, Texas (MAF); and Brownsville, Texas (BRO); for three times during the surge event. Figure 10 shows the locations of these soundings.

At 0000 UTC 12 November the surge had passed only RAP, where strong north-northwest flow near the surface backed to northwesterly aloft. Ahead of the surge at DDC, the winds veered from southerly to west-

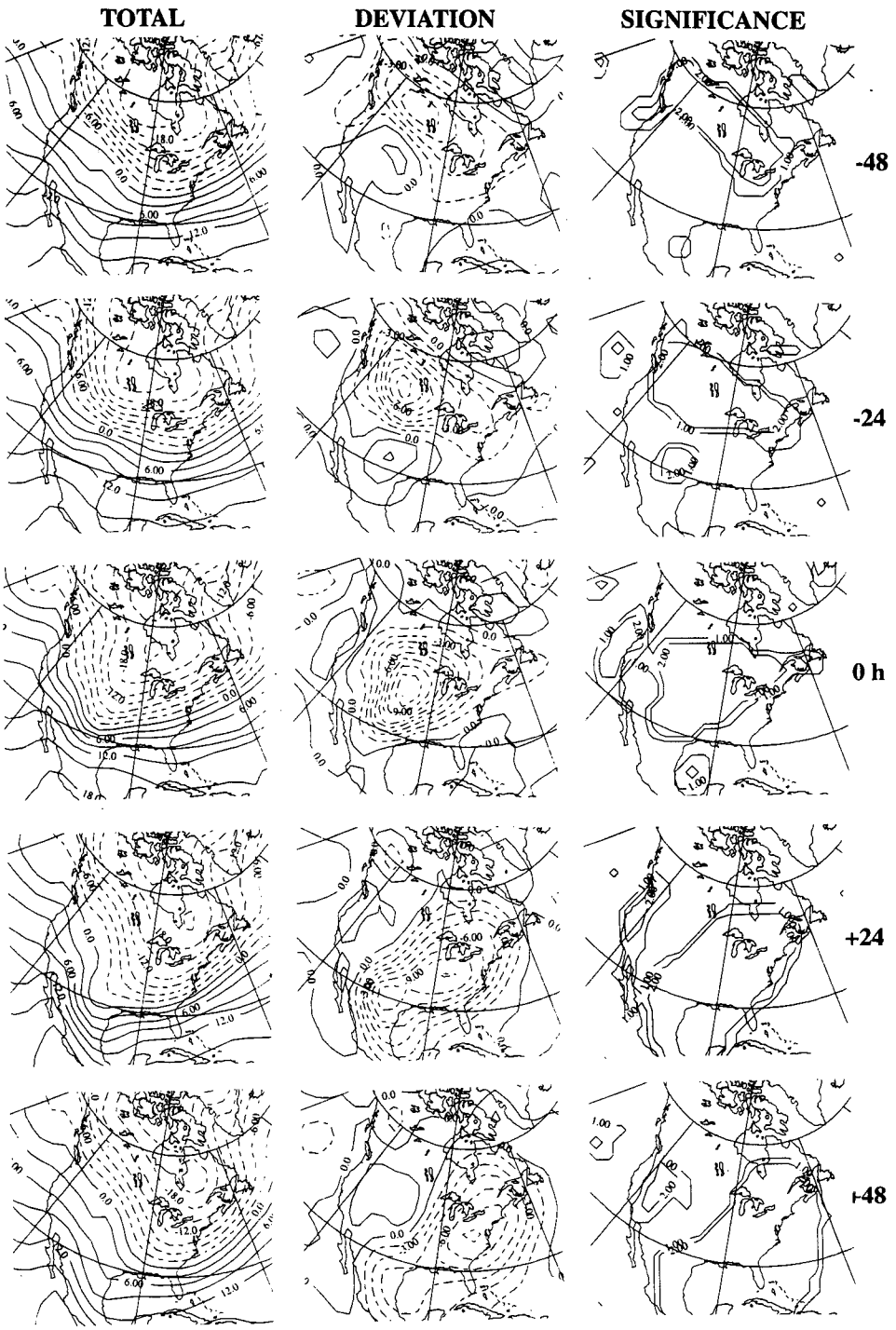

FIG. 4. Temperatures, temperature deviations from climatology at 850 mb, and statistical significance of the deviations for the composite event. The contour intervals are 3°C for the total composites and 1.5°C for the deviations. Significance levels of 95% and 99% are indicated by 1.00 and 2.00, respectively.

northwesterly with height; an inversion between 850 and 800 mb and a dry layer above 850 mb were associated with the westerly, subsiding flow. At MAF, a dry-adiabatic surface layer was surmounted by a deep inversion–isothermal layer. The sounding at BRO had moderate northerlies near the surface from a previous surge event. The northerlies were capped by an inversion and saturated upslope northeasterly flow.

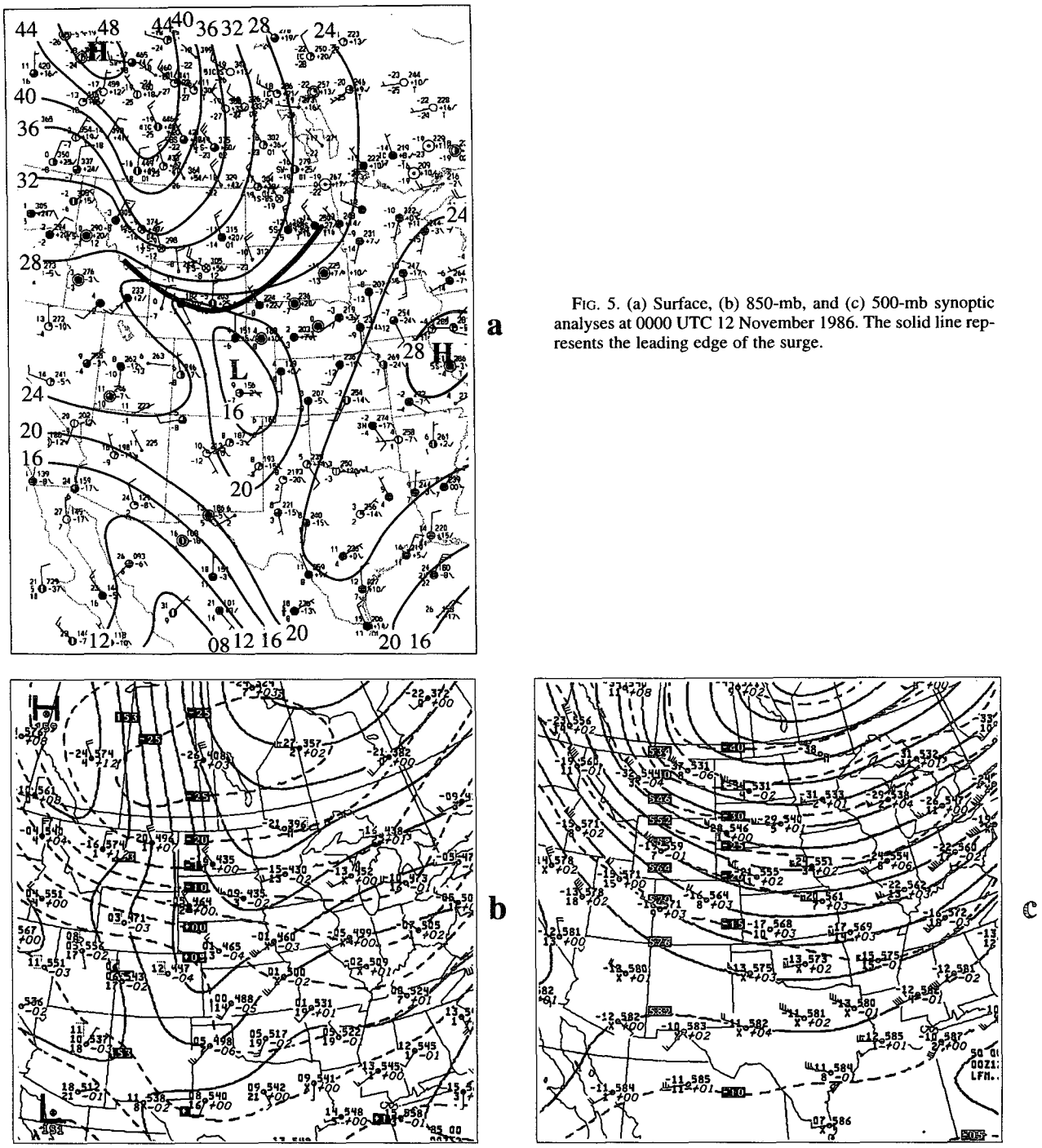

FIG. 5. (a) Surface, (b) 850-mb, and (c) 500-mb synoptic analyses at 0000 UTC 12 November 1986. The solid line represents the leading edge of the surge.

By 0000 UTC 13 November the effects of the northerly surge are seen in all the soundings except BRO. The sounding at RAP was very cold (about 16°C near the surface), with southwesterly flow at low levels (due to the southeastward movement of the anticyclone), northwesterly flow aloft increasing with height, and a stable, nearly isothermal layer extending to approximately 600 mb. At DDC, strong northerly flow near the surface backed to northwesterly above an inversion at 840–810 mb. The sounding at MAF shows the typical vertical structure associated with a recent passage of a cold surge along the Rockies. Strong upslope north-

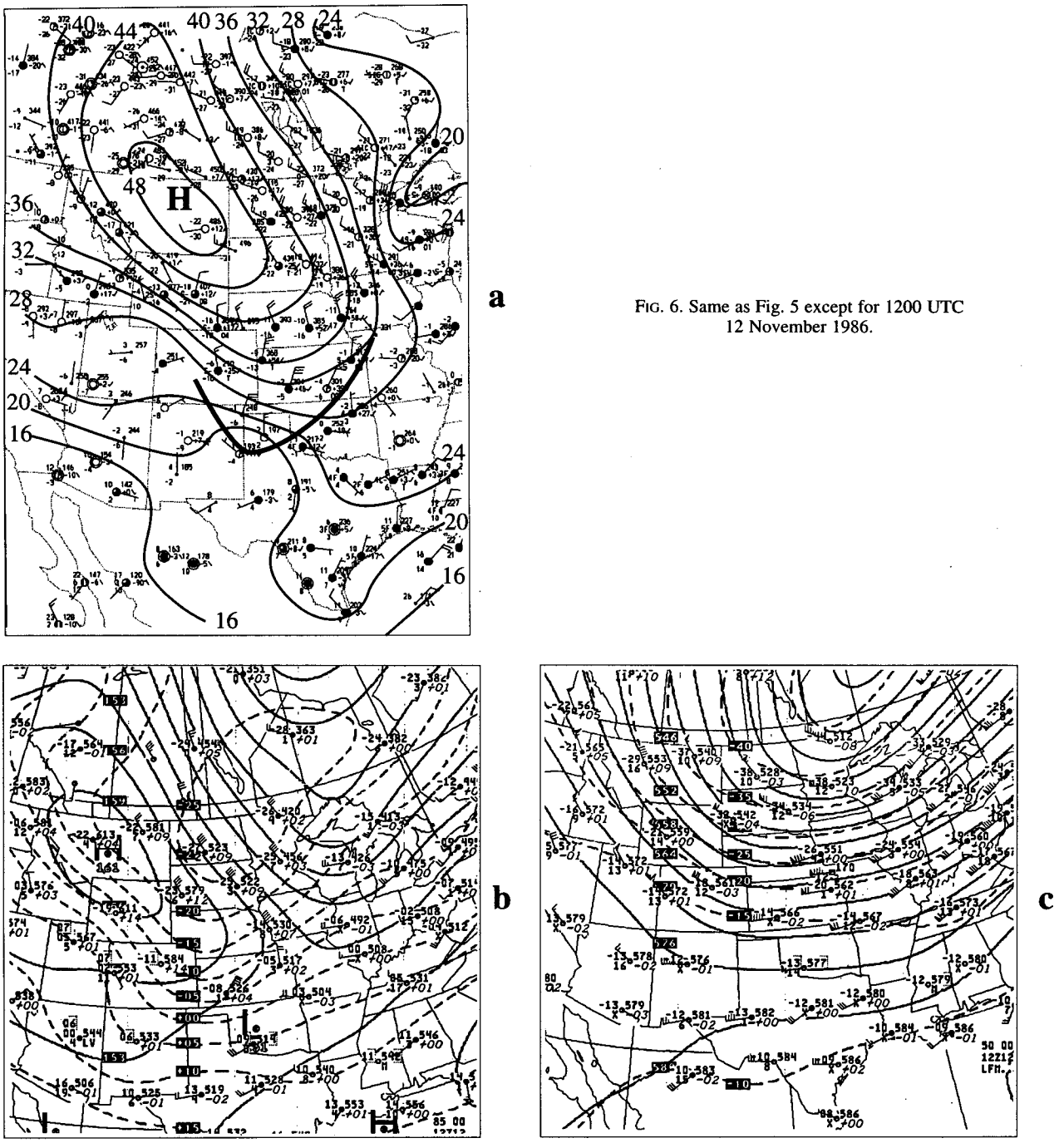

FIG. 6. Same as Fig. 5 except for 1200 UTC 12 November 1986.

easterlies and saturated conditions were observed below an inversion that was located at or below the crest of the Rockies to the east. Above the inversion, the winds switched rapidly into the southwest. Finally, south of the surge at BRO, there are north/northwesterly winds and a weak inversion below 950 mb from the lingering shallow cold dome of the previous surge event.

By 0000 UTC 14 November, subsidence associated with downslope flow and the synoptic anticyclone led to dramatic warming and a surface-based inversion at RAP. At DDC the winds had become southerly, with a deep inversion above a well-mixed surface layer. A strong inversion between 880 and 800 mb was still present at MAF as the cold dome remained entrenched across the southern plains. The cold surge had finally

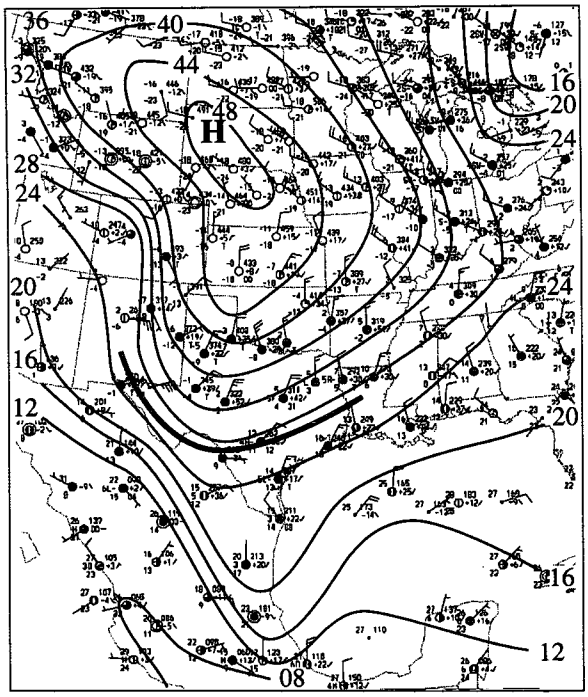

a

FIG. 7. Same as Fig. 5 except for 0000 UTC 13 November 1986.

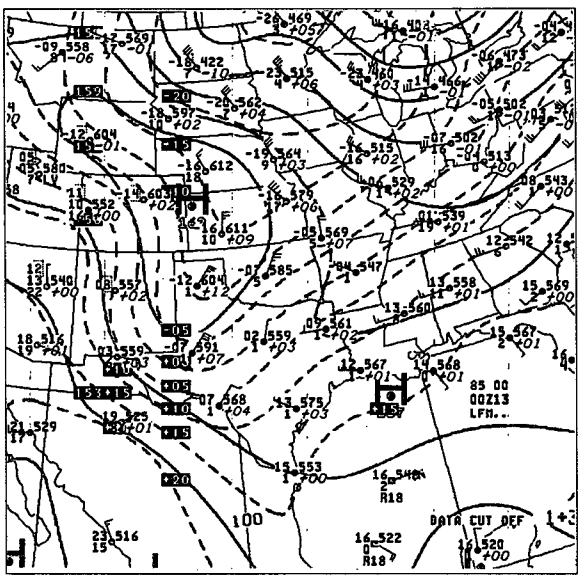

b

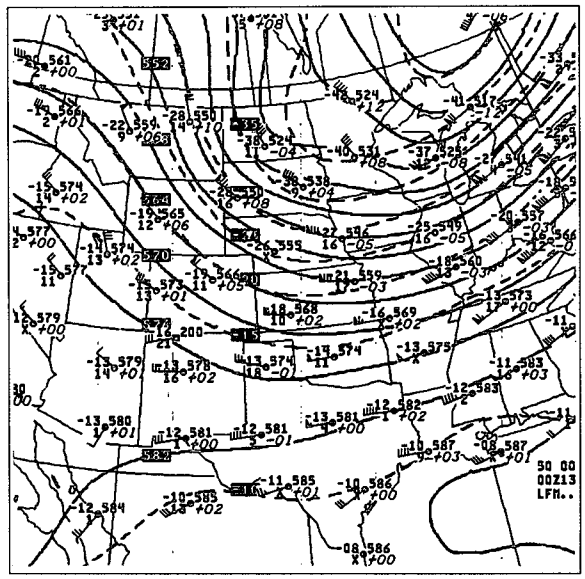

c

reached BRO, where strong northwesterly flow was capped by a low-level inversion.

c. *Time series*

Time series of surface observations at North Platte, Nebraska (LBF); San Angelo, Texas (SJT); and Brownsville, Texas (BRO); are displayed in Fig. 11.[5]

At 0000 UTC 12 November the cold surge was located about 200 km north of North Platte (cf. Fig. 5a). Weak northerlies began there around 0100 UTC, but the strongest northerlies and largest temperature falls arrived 2 h later. By 1500 UTC 12 November, the temperature at North Platte had dropped nearly 15°C, and the pressure had risen about 25 mb since 0000 UTC 12 November. Subsequently, the pressure fell rapidly as the winds turned southerly and temperatures increased.

At San Angelo, the pressure began to rise, and a gradual clockwise wind shift occurred a few hours be-

[5] Figure 10 shows the locations of these stations.

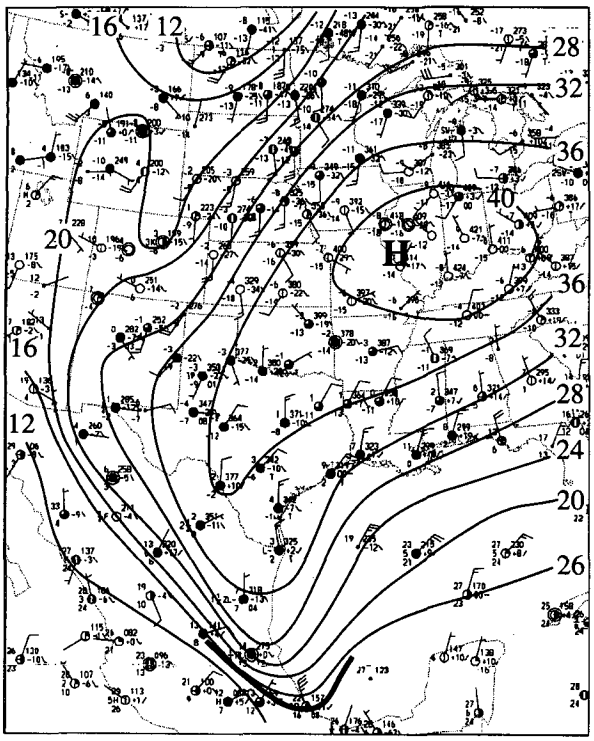

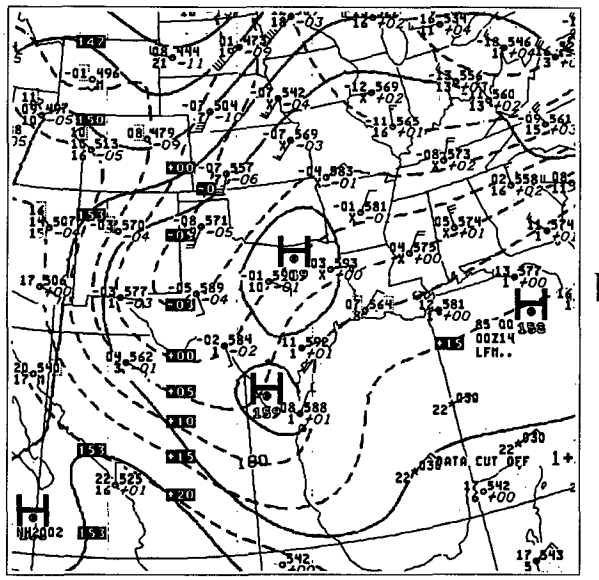

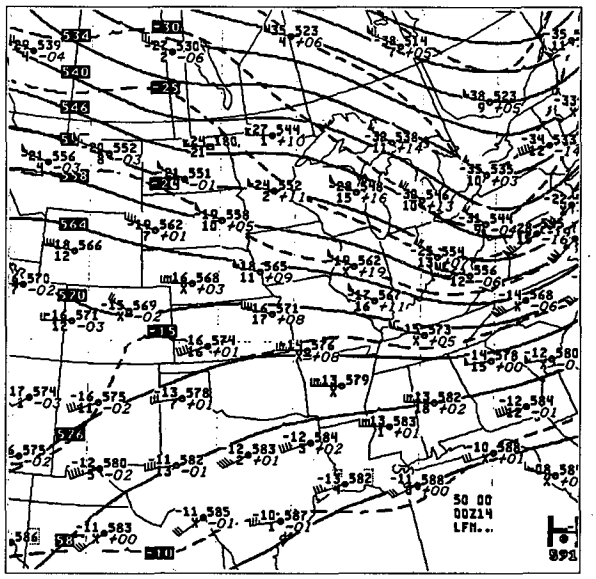

FIG. 8. Same as Fig. 5 except for 0000 UTC 14 November 1986.

fore the arrival of strong northerlies, as a result of the southward movement of the weakening lee trough. The temperature rose dramatically as winds and vertical mixing increased around 1800 UTC 12 November. A shift to strong northerlies and a rapid temperature drop around 1900 UTC 12 November accompanied surge passage during which the temperature dropped approximately 20°C and the pressure rose 20 mb within 24 h.

The surge passage at Brownsville, Texas, was relatively subtle, as northwesterly winds exceeding 10 kt (5 m s^{-1}) occurred throughout the entire 48-h period. Only diurnal pressure and temperature variability were observed during most of 12 November. At 2200 UTC 12 November the pressure started to rise; the rate of pressure rise increased after 0600 UTC 13 November when the temperature began to fall more rapidly. Similar transitions were common along the Mexican coast.

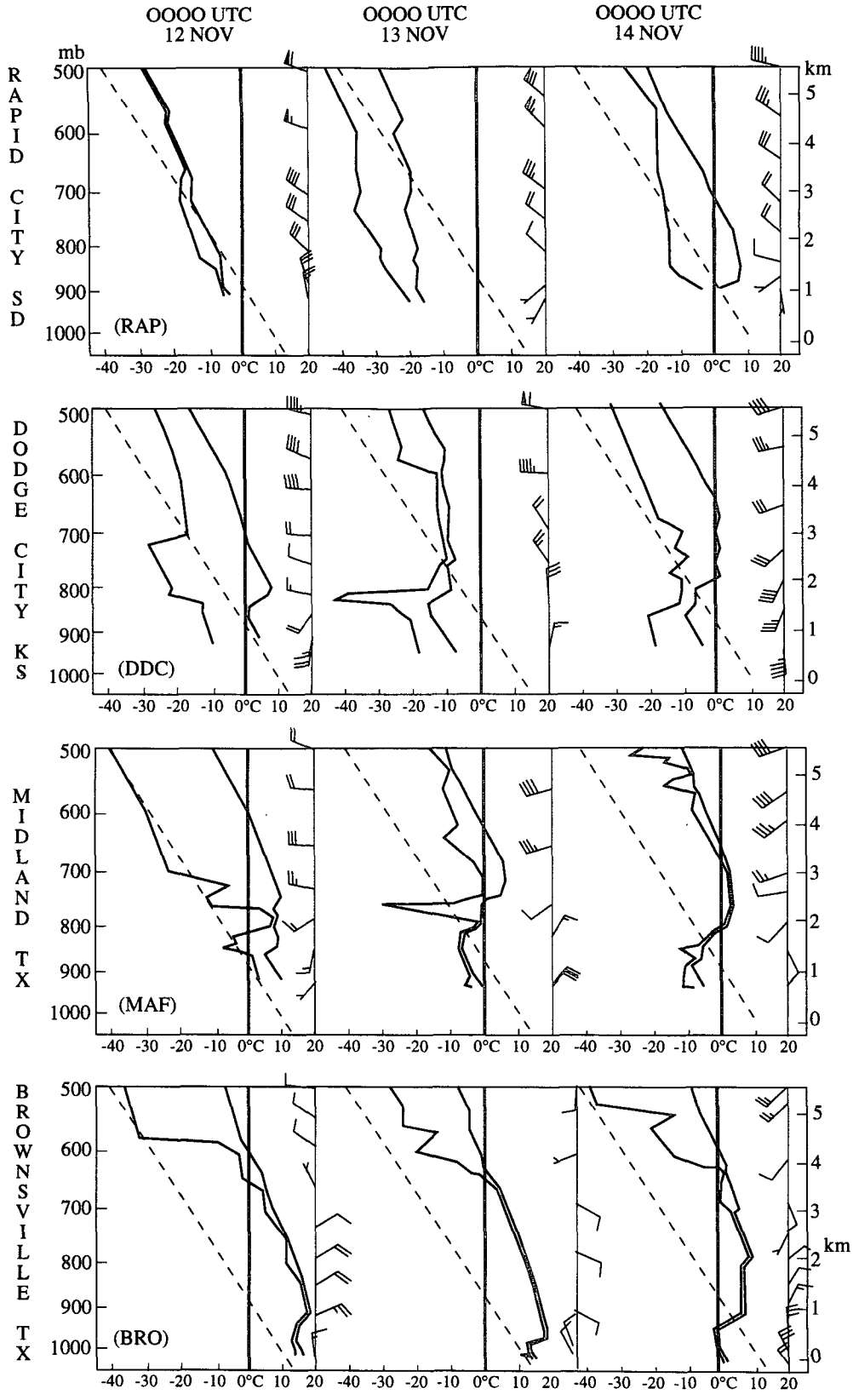

FIG. 9. Soundings for Rapid City, South Dakota (RAP); Dodge City, Kansas (DDC); Midland, Texas (MAF); and Brownsville, Texas (BRO); at 0000 UTC 12, 13, and 14 November 1986. The dashed line indicates a dry adiabat.

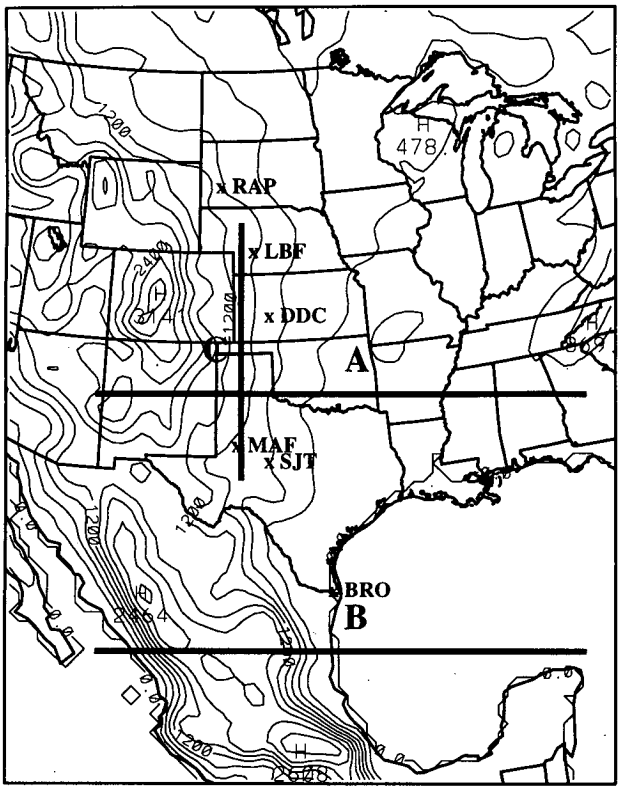

FIG. 10. Model topography contoured every 300 m. Lines A–C represent the vertical cross-section positions, and the crosses represent sounding and/or time series locations.

4. Simulation verification and model description of the 12–14 November 1986 case

a. *Description of the mesoscale model*

The Penn State–National Center for Atmospheric Research (PSU–NCAR) Mesoscale Model Version 4 (MM4) was used to simulate and provide the detailed data necessary to diagnose the 12–14 November 1986 surge event. The MM4 is a hydrostatic, primitive equation, sigma-coordinate model (Anthes and Warner 1978; Anthes et al. 1987). An explicit moisture scheme (Hsie 1984) featuring only liquid and vapor precipitation physics was used with an implicit cumulus parameterization (Grell et al. 1988). A cloud radiative feedback parameterization described by Benjamin (1983) was included. The planetary boundary layer (PBL) was parameterized using the approach of Zhang and Anthes (1982).

The simulations for this event used 24 vertical full-sigma levels,[6] a horizontal grid spacing of 45 km, and were integrated for 48 h. Analyses at the surface and aloft at 12-h intervals, required for the initial and boundary conditions, were constructed by interpolating the NMC global analyses to the model grid and then using a Cressman scheme to improve the analyses with observations. These analyses were linearly interpolated in time to provide the model's boundary conditions. The model topography (Fig. 10) was derived using the Cressman analysis scheme and a 1–2–1 smoother on 10-min-averaged terrain.

Two simulations were made, one with and the other without four-dimensional data assimilation (FDDA).[7] Both simulations were initialized at 0000 UTC 12 November. The simulation that applied FDDA nudged the winds and moisture within the planetary boundary layer (PBL) and the temperature and winds above the PBL for the first 12 h of the simulation, after which FDDA was not used. This approach provided a more realistic simulation during the latter part of the integration. However, since FDDA results in unphysical terms in the prognostic equations, all model-derived diagnostics and figures during the first 12 h of the surge (0000–1200 UTC 12 November) are based on the non-FDDA simulation, whereas the FDDA simulation is used for all times following 1200 UTC 12 November.

b. *Horizontal evolution*

Figure 12 shows the model sea level pressure, temperature, and wind fields at the surface[8] at 0600 UTC 12 November 1986. At this time, 6 h after model initialization, the leading edge of the surge extended northeastward from northeast Colorado to Iowa. The winds within the surge were primarily downgradient. The lee low, located over the northeast corner of New Mexico, was slightly (~2 mb) overdeveloped by the model. Diagnosing vertical velocity (not shown) indicated that the troughing was forced by downslope adiabatic warming on the lee side of the Rockies. The overdevelopment of the trough was probably caused by anomalously strong northwesterly winds near the surface (approximately 15 m s^{-1} in the model compared to 8 m s^{-1} observed) over the high terrain, which in turn generated excessive downslope warming and troughing. An upslope component existed just to the north of the leading edge of the surge.

Figure 13 shows the surface, 850-mb, and 500-mb model fields at 1200 UTC 12 November. At low-levels, the model produced excessive warming and lee troughing (by about 8°C and 5 mb, respectively) over the

[6] The full-sigma levels were σ = 1.0, 0.99, 0.98, 0.96, 0.93, 0.89, 0.85, 0.8, 0.75, 0.7, 0.65, 0.6, 0.55, 0.5, 0.45, 0.4, 0.35, 0.3, 0.25, 0.2, 0.15, 0.1, 0.05, 0.00.

[7] The FDDA scheme applies Newtonian relaxation to nudge the model state toward the NMC 3-h surface and 12-h upper-air gridded analysis (Stauffer and Seaman 1990).

[8] The surface fields in Fig. 12, as well as in subsequent figures, are for the model's lowest half-sigma level (σ = 0.995), which is located approximately 40 m above the surface.

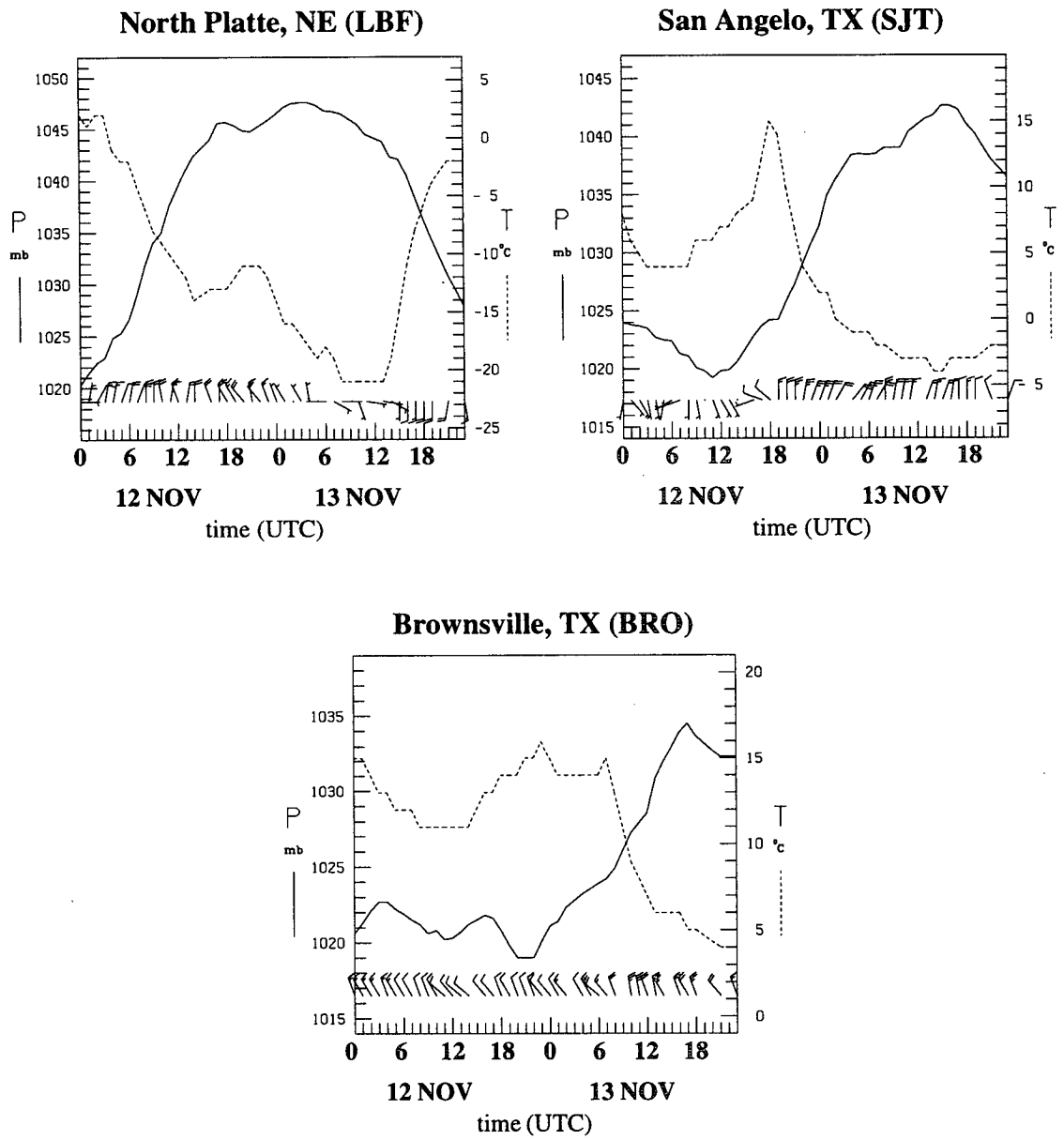

FIG. 11. Time series from 0000 UTC 12 November to 0000 UTC 14 November 1986 at North Platte, Nebraska (LBF); San Angelo, Texas (SJT); and Brownsville, Texas (BRO). Pressure (solid) is in millibars, and temperature (dashed) is in degrees Celsius. The locations of the stations are shown in Fig. 10.

Texas panhandle and eastern Oklahoma (Figs. 13a,b), resulting in an unrealistically large temperature gradient at the leading edge of the surge at the surface. The other structures, such as the along-barrier cold tongue at 850 mb and strong northerlies at the surface and 850 mb behind the leading edge of the surge were better represented. The structure at 500 mb was realistic, with the axis of the upper-level trough extending from Colorado northeastward into Minnesota.

During the next 12 h, the lee trough dissipated and the leading edge of the surge moved southward across western Texas. By 0000 UTC 13 November, the leading edge of the simulated cold surge at the surface and 850 mb was over the Texas–Mexican border (Figs. 14a,b), close to the observed position (Fig. 7). The winds were highly ageostrophic over most of the cold outbreak region, both adjacent to and away from the Rockies. Temperature gradients were strongest over the sloping terrain of southern New Mexico and southwestern Texas. Calculations of three-dimensional Lagrangian frontogenesis at the surface for this time (not shown) indicate strong frontogenesis over these steep

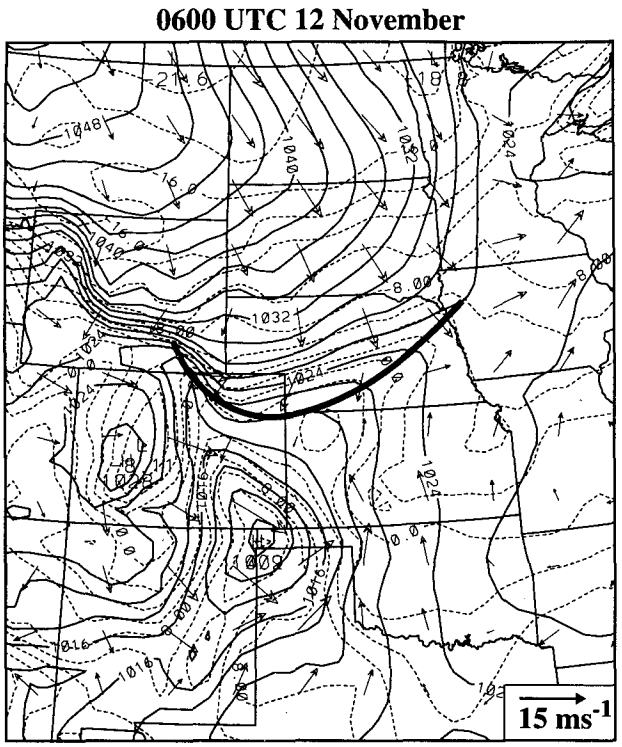

FIG. 12. Model surface analysis at 0600 UTC 12 November 1986 showing sea level pressure (every 2 mb), temperature (every 2°C), and wind vectors. The solid line indicates the leading edge of the surge.

slopes resulting from the confluence and deformation of the blocked upslope flow. Although the temperature gradients were intense at the surge's leading edge, a sharp directional shift from southerly to northerly winds did not exist there; rather, there was a rapid increase in the speed of the northerlies. At 850 mb, a tongue of cold air extended southward over the southern plains. The model captured the structures of the surface and 850-mb ridging well, but the intensity of the ridging was slightly stronger than observed. Structures at 500-mb were well represented in the model (Fig. 14c).

At 0600 UTC 13 November, the leading edge of the surge extended from south of the Texas and Louisiana coasts to across the northern Mexico coast (Fig. 15). The surge was not associated with a sharp wind direction transition since northerlies existed in advance of the leading edge. South of the primary surge over the open waters of the gulf, there was a secondary wind shift associated with a previous weaker surge. Pressure ridging, with a noticeably smaller scale than over central Texas (a few hundred kilometers versus a thousand kilometers), had formed along the Mexican coast. An intense surface baroclinic zone existed along the U.S. gulf coast due to the rapid modification of the cold continental air over the warm gulf waters. Another baroclinic zone was developing along the Mexican coast because of the contrast in temperatures between air parcels moving over the cold land and the warmer water to the east.

By 0000 UTC 14 November, as in the observed field (Fig. 8a), the main anticyclone (1046 mb) had moved eastward with the upper-level ridge that was embedded in the "steering flow" aloft (Fig. 16d), and a tongue of high pressure remained behind over the southern plains and the Mexican coast (Figs. 16a,b). Model pressures and heights were slightly higher at the surface and 850 mb than observed (by about 5 mb and 30 m, respectively). The surface ridge over coastal Mexico reached its maximum southward extent at this time (Fig. 16b) and was well simulated by the model. The winds within the coastal ridge were highly ageostrophic and generally had a greater downgradient component than the winds over the gulf. At 850 mb, the coastal temperature gradient was much weaker, and the winds were more geostrophic than at the surface (Fig. 16c).

c. *Vertical structure and evolution of the leading edge of the cold surge*

As the surge moved southward along the sloping terrain, its vertical structure changed dramatically. To show this, Fig. 17 presents a time series of vertical cross sections along the eastern slopes of the Rockies (line C on Fig. 10 shows the location of the sections). At 6 h into the (non FDDA) simulation (0600 UTC 12 November), the surface position of the lee trough (LT) was coincident with a dip in the isentropes at low levels (most of the lee troughing and warm anomaly was west of the section). Two baroclinic zones were present, one immediately north of the lee trough and another associated with the leading edge of the surge (at point S).

By 12 h into the (non-FDDA) simulation (1200 UTC 12 November), strong northerlies ($\sim$20 m s^{-1}) extended southward to the Texas panhandle. The strong winds to the north of the Texas panhandle developed in situ as a result of the increasing north–south pressure gradient between the weak surface trough over the Texas panhandle and the anticyclone to the north (cf. Fig. 13). The two baroclinic zones present at 0600 UTC 12 November were beginning to merge. Because of this merging and the development of continuous strong northerlies behind the lee trough, the leading edge of the surge at the surface (S) could now be placed within the trough axis.

By 18 h into the FDDA simulation (1800 UTC 12 November), the forward part of the surge had become more shallow, with the strongest northerlies (>10 m s^{-1}) limited to the layer below 850 mb. Mechanical mixing behind the surge had deepened the surface mixed layer within the colder air, and the stability had increased above this layer. A sharp transition from southerly to northerly winds was not coincident with the strong baroclinic zone associated with the leading edge of the surge.

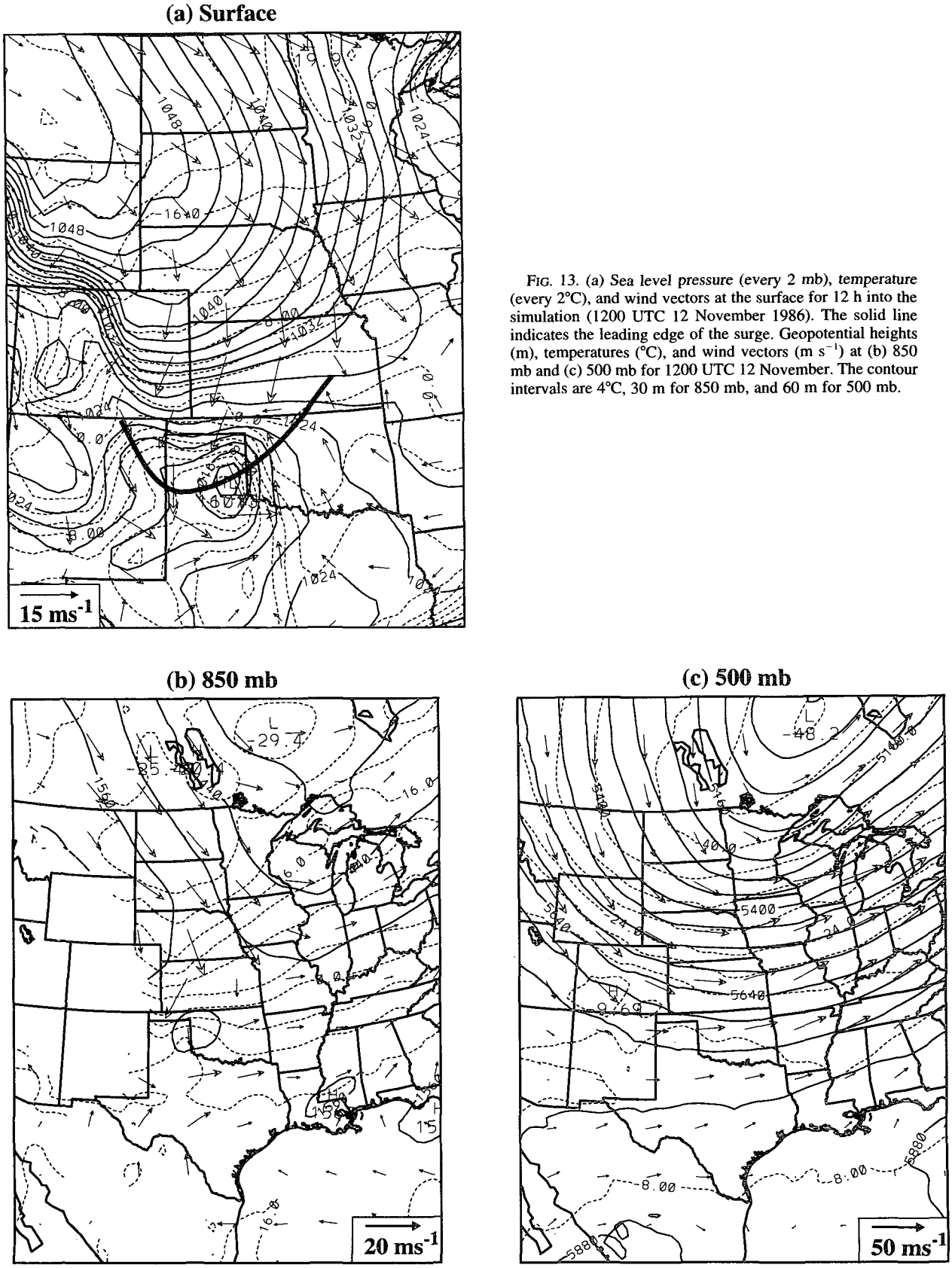

FIG. 13. (a) Sea level pressure (every 2 mb), temperature (every 2°C), and wind vectors at the surface for 12 h into the simulation (1200 UTC 12 November 1986). The solid line indicates the leading edge of the surge. Geopotential heights (m), temperatures (°C), and wind vectors (m s^{-1}) at (b) 850 mb and (c) 500 mb for 1200 UTC 12 November. The contour intervals are 4°C, 30 m for 850 mb, and 60 m for 500 mb.

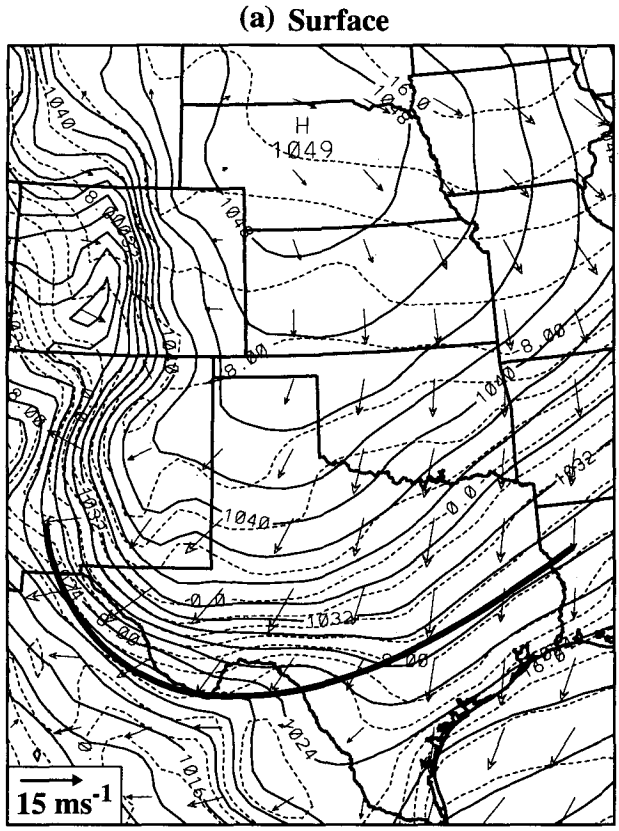

FIG. 14. Same as Fig. 13 except at 0000 UTC 13 November 1986 (24 h into the simulation).

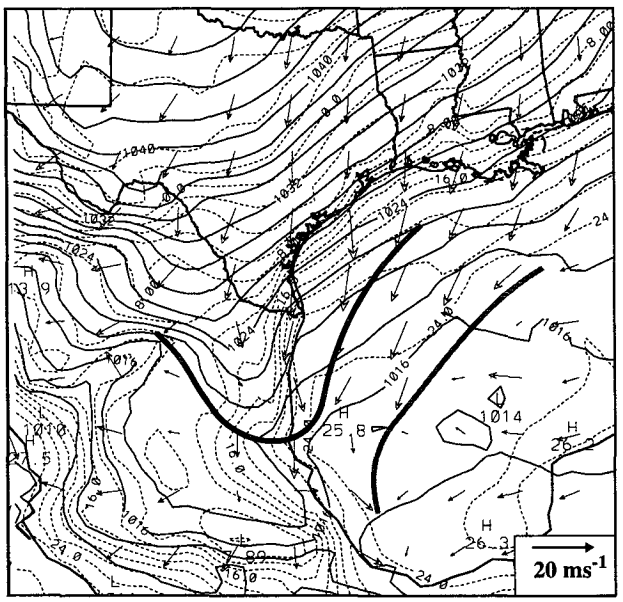

FIG. 15. Model surface analysis for 0600 UTC 13 November 1986 showing sea level pressure (every 2 mb), temperatures (every 2°C), and wind vectors. The northern line indicates the leading edge of the surge, while the southern line indicates a preexisting stationary frontal boundary.

d. *Cold dome structure and evolution*

An important feature of the cold surge was the damming of cold air by the sloping terrain (Figs. 14a,b). To illustrate this phenomena, Fig. 18 provides model cross sections taken normal to the Rockies showing the meridional wind component and potential temperature at 6, 18, 30, and 42 h into the simulation (corresponding to 0600 and 1800 UTC on 12 and 13 November). The bold lines A and B on Fig. 10 show where the sections are taken.

At 0600 UTC 12 November, the surge was still located to the north of section A, with a preexisting cold stable layer over the lower slopes; a slight dip in the isentropes over the upper portions of the slope indicates the low-level warm anomaly and lower stability associated with lee troughing. By 1800 UTC 12 November, there was considerable evidence of cold-air damming in section A, with tilting isentropes and a northerly low-level jet ($\sim$16–22 m s^{-1}) centered between 900 and 850 mb over the sloping terrain. As in Fig. 17, nearly vertical isentropes near the surface show that the strong northerlies behind the surge resulted in vertical mixing. Twelve hours later at 0600 UTC 13 November, the northerly jet had split, with one branch associated with the retreating synoptic-scale anticyclone separating itself from a terrain-bounded jet. By 1800 UTC 13 November, the cold air was still firmly entrenched over the sloping terrain of section A; although the cores of the northerly low level jets had moved eastward, northerlies still extended westward up the slope. Meanwhile, over the steeper upper slopes of section A, the southerly wind maxima ($\sim$10–15 m s^{-1}) increased.

Initially (0600 UTC 12 November) in section B, weak cold-air damming was evinced by tilting isentropes and a low-level northerly jet adjacent to the barrier. By 1800 UTC 12 November, the low-level northerlies had strengthened along the Mexican coast to approximately 22 m s^{-1}. Twelve hours later (0600 UTC 13 November), the surge was approaching section B (cf. Fig. 15), and the northerly low-level jet and narrow cold dome were still present along the Mexican coast. Finally by 1800 UTC 13 November, damming and northerlies had greatly increased over coastal Mexico, with the width of the damming noticeably narrower in this region than over the Great Plains.

5. Model diagnostics

a. *Thermodynamic energy equation*

The magnitude of the terms of the thermodynamic energy equation were diagnosed to determine the origins of the local temperature changes during the evolution of the surge. If adiabatic cooling caused by upslope flow at the leading edge of the surge is the dominant process in extending the anticyclone southward, this would suggest topographic Rossby wave characteristics. In contrast, the domination of advection would be indicative of damming or trapped gravity current dynamics.

Ignoring diabatic effects and vertical advection, the thermodynamic energy equation in an isobaric vertical coordinate system can be written

$$\frac{\partial T}{\partial t} = -u\frac{\partial T}{\partial x} - v\frac{\partial T}{\partial y} + \omega\left(\frac{\alpha}{c_p} - \frac{\partial T}{\partial p}\right), \qquad (1)$$

where u and v are the horizontal wind components in the zonal and meridional directions, T is temperature, p is pressure, c_p is isobaric specific heat, and α is specific volume. The local change was approximated by centered time differences (Δt = 30 min). The horizontal advection term was calculated using centered differencing on pressure surfaces, with the results being interpolated back to sigma surfaces. Figure 19 shows the contributions of the various terms in (1) averaged over the lowest five half-sigma layers in the model (the 75-mb layer above the surface) at 0600 UTC and 1800 UTC 12 November, and 1200 UTC 13 November 1986.

At 6 h (0600 UTC 12 November) the leading edge of the northerly surge, associated with local temperature cooling exceeding 2.5 $\times$ 10^{-4} °C s^{-1}, stretched from Nebraska into northeastern Colorado and southern Wyoming. Over the plains, most of this local cooling was induced by cold advection, while over the southern slopes of Wyoming and eastern Colorado, adiabatic cooling (forced by upslope flow) was also sig-

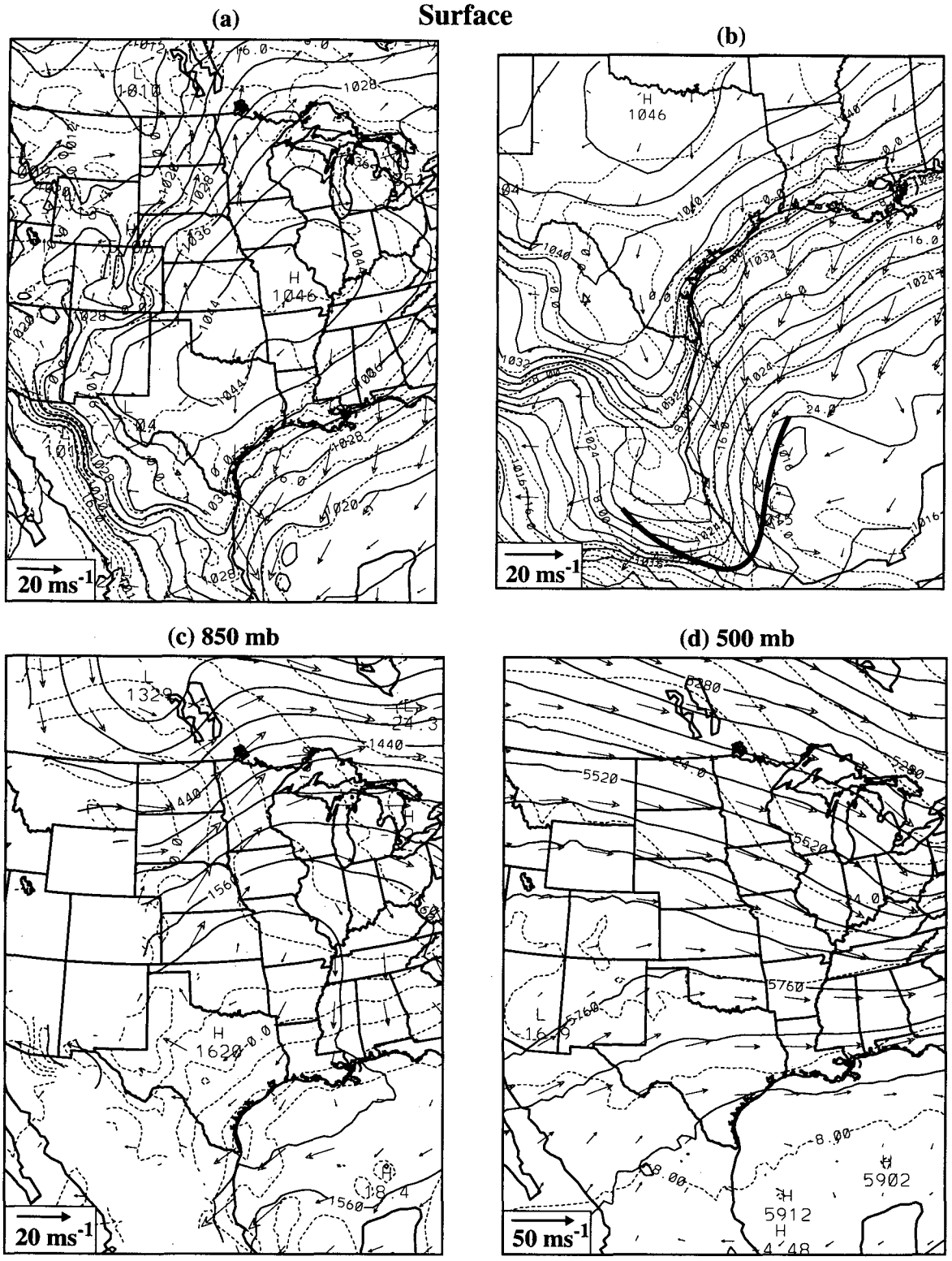

FIG. 16. (a) Sea level pressure (every 4 mb), temperature (every 4°C), and wind vectors (m s^{-1}) at the surface for 48 h into the simulation (0000 UTC 14 November 1986). (b) Model surface analysis for 0000 UTC 14 November 1986 showing sea level pressure every 2 mb, temperature every 2°C, and surface wind vectors in meters per second. The solid line indicates the leading edge of the surge. Geopotential heights (m), temperatures (°C), and wind vectors at (c) 850 mb and (d) 500 mb, respectively, for 0000 UTC 14 November using contour intervals of 4°C, 30 m for 850 mb, and 60 m for 500 mb.

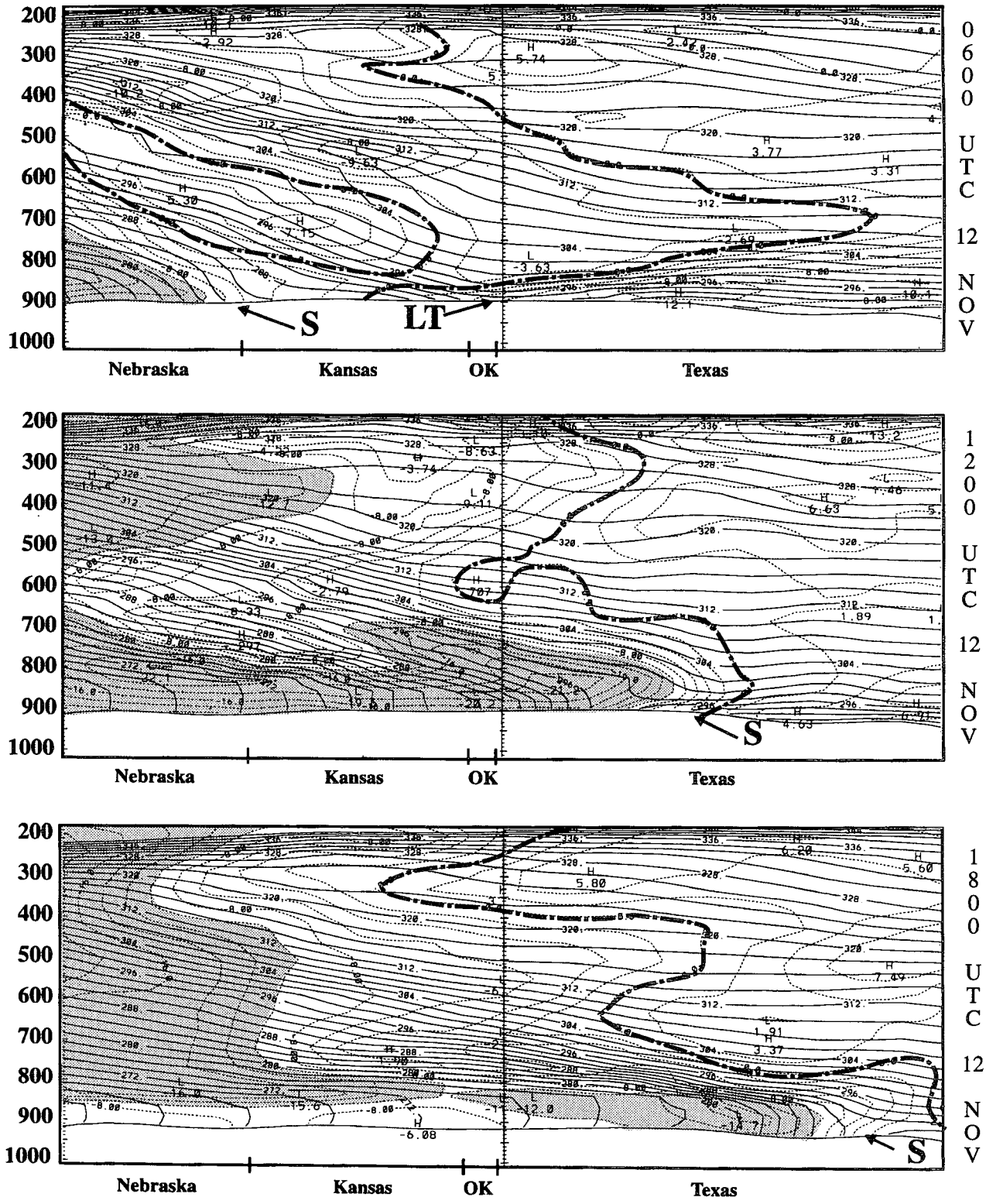

FIG. 17. Vertical cross section parallel to the Rockies of potential temperature (solid every 2 K) and the meridional wind component (dashed, every 2 m s^{-1}) for 0600, 1200, and 1800 UTC 12 November 1986. The cross-section location is shown by line C in Fig. 10. The heavy dashed line represents the zero line in the northerlies, and the shading shows winds in excess of 10 m s^{-1}.

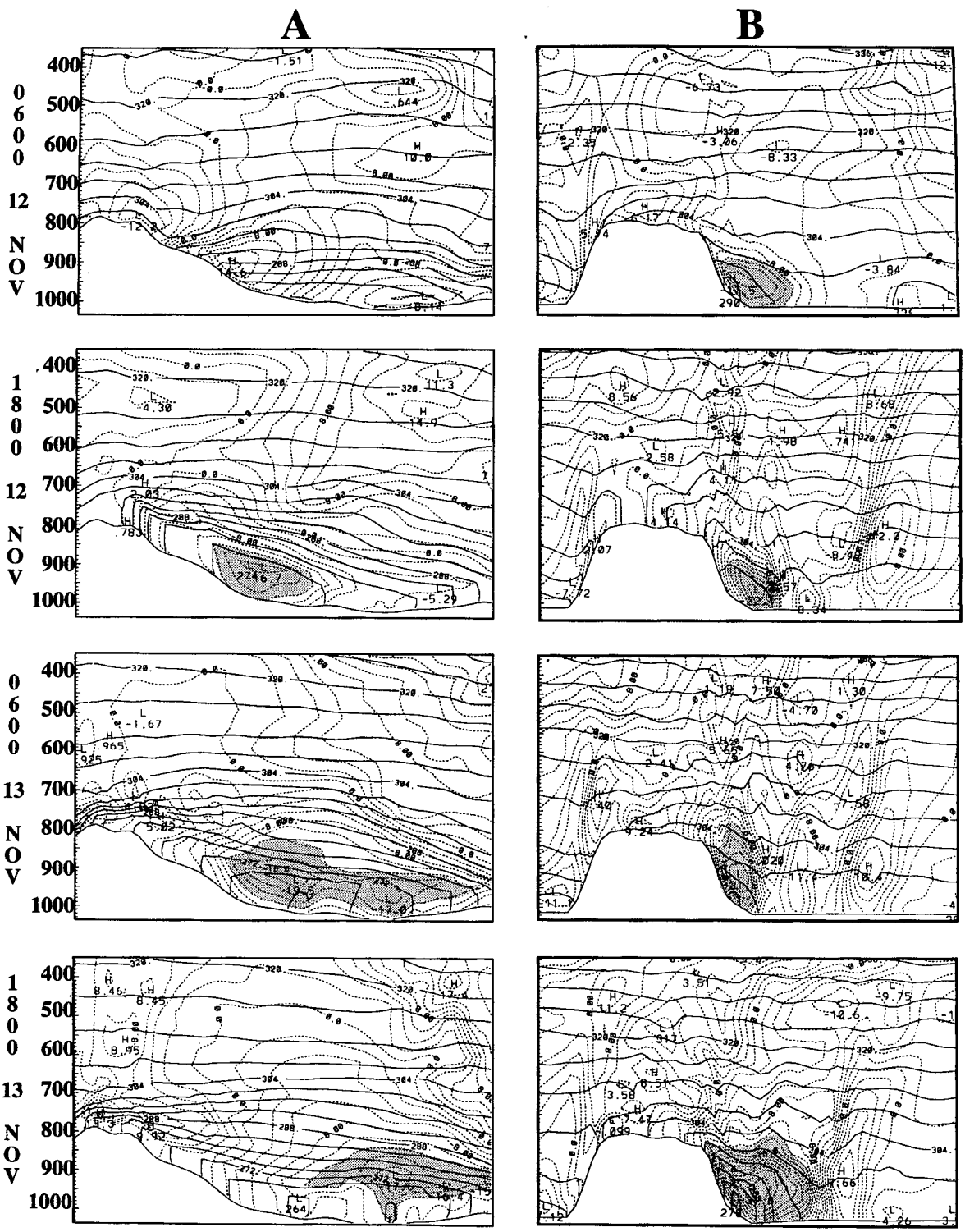

FIG. 18. A series of cross sections showing both potential temperature (solid every 4 K) and the meridional wind component (dashed every 2 m s^{-1}) at 0600 and 1800 UTC 12 November, and 0600 and 1800 UTC 13 November 1986. The cross-section locations, A and B, are shown in Fig. 10. The shading indicates winds equal to or greater than 12 m s^{-1}.

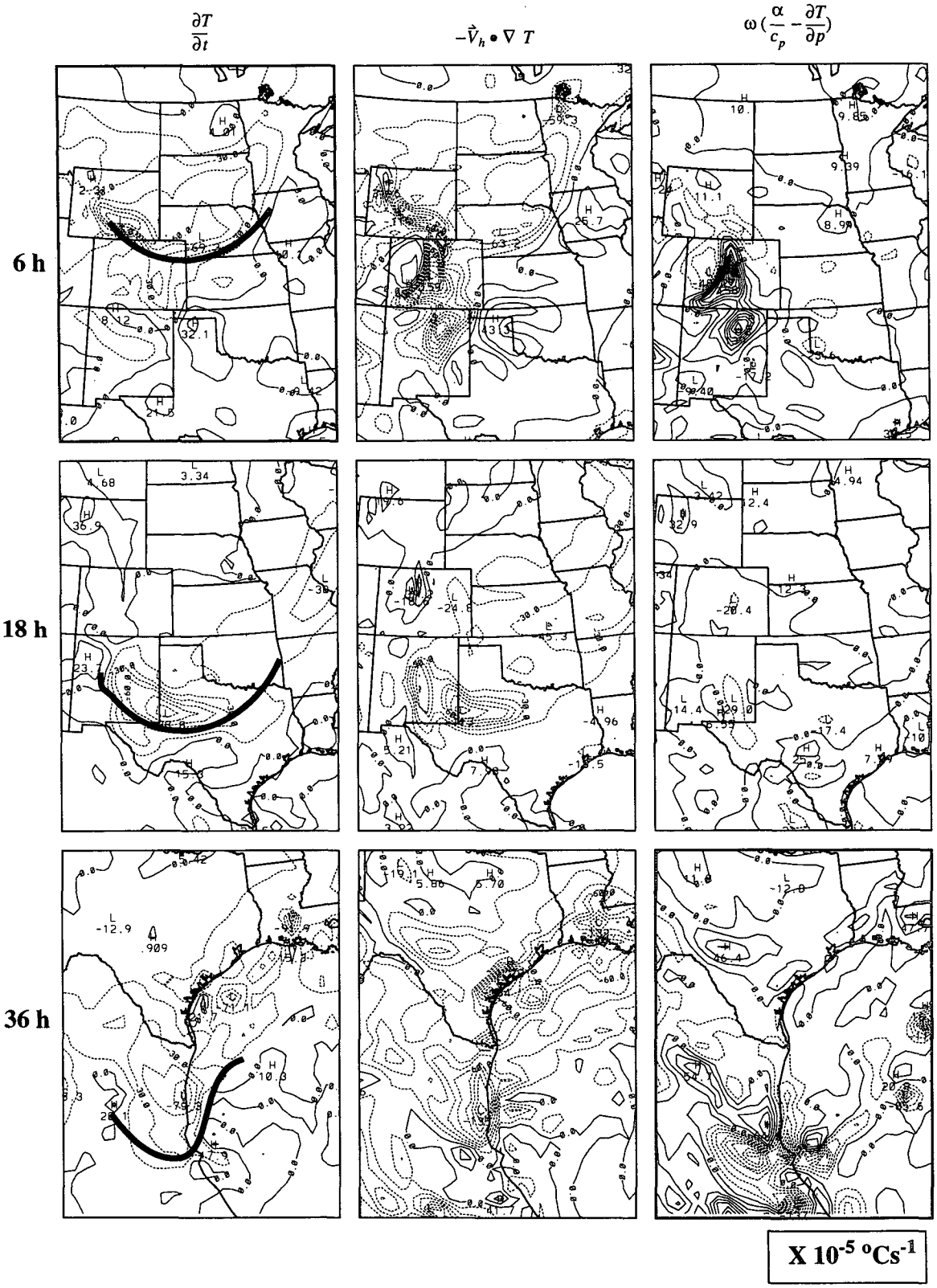

FIG. 19. Diagnosis of the thermodynamic energy equation showing the local temperature change, horizontal advection, and the adiabatic terms averaged for the lowest five half-sigma levels (~75-mb layer) at 6, 18, and 36 h into the simulations (0600 and 1800 UTC 12 November and 1200 UTC 13 November 1986, respectively). The contour interval is 1.5×10^{-4} °C s^{-1}.

nificant. However, even on these slopes, cold advection was two to three times greater than adiabatic cooling. Also at 0600 UTC, strong adiabatic warming ($\sim 8.0 \times 10^{-4}$ °C s^{-1}) caused by downslope flow was coincident with the area of troughing over eastern New Mexico and the eastern slopes of the Colorado Rockies.

By 18 h (1800 UTC 12 November), the largest local cooling ($< -4.0 \times 10^{-4}$ °C s^{-1}) was found over the sloping terrain of western Texas and New Mexico. Cold advection was clearly dominant over adiabatic cooling.

By 36 h (1200 UTC 13 November) the northerly surge had reached coastal Mexico, with local cooling along the Mexican coast. Nearly all the cooling north of the leading edge of the surge was caused by strong cold advection ($< -4 \times 10^{-4}$ °C s^{-1}), with another area of strong cold advection along the Texas and Louisiana coasts. In contrast, only weak cold advection was occurring immediately behind the front over the gulf, because strong surface sensible heating had reduced the temperature gradients. Adiabatic cooling was strong immediately ahead of the surge along the Mexican coast because of enhanced low-level upward motion induced by frontal convergence and upslope flow.

In summary, adiabatic cooling caused by upslope flow at the leading edge of the surge was generally much smaller than horizontal cold advection. This result is not consistent with topographic Rossby or shelf wave dynamics and is suggestive of damming or a trapped density current.

b. Vorticity equation

The vorticity equation was used to determine whether anticyclonic tendencies moved south because of advection or as a result of upslope flow at the leading edge of the surge causing air columns to contract. Dominance of the latter mechanism would be consistent with the topographic Rossby wave mechanism. The vertical advection, tilting, and the solenoidal terms were generally found to be much smaller than other terms in the vorticity equation; therefore, those terms will be ignored here. The remaining terms for the isobaric vorticity equation can be written:

$$\frac{\partial \zeta}{\partial t} = -\mathbf{V}_h \cdot \nabla(\zeta + f) + (\zeta + f)\frac{\partial \omega}{\partial p} + \left(\frac{\partial F_y}{\partial x} - \frac{\partial F_x}{\partial y}\right), \quad (2)$$

where the first term on the right-hand side is the advection of absolute vorticity, the second is the generation or divergence term caused by differential vertical motion, and the last term is the vorticity generated by horizontal gradients of friction. Friction[9] was estimated from the residual of the momentum equations:

$$F_x = \frac{\partial u}{\partial t} + u\frac{\partial u}{\partial x} + v\frac{\partial u}{\partial y} - fv + g\frac{dz}{dx}, \quad (3)$$

$$F_y = \frac{\partial v}{\partial t} + u\frac{\partial v}{\partial x} + v\frac{\partial v}{\partial y} + fu + g\frac{dz}{dy}. \quad (4)$$

All the terms in (2), (3), and (4) were averaged for the five lowest half-sigma levels ($\sim$75-mb layer from the surface upward), and the local changes were approximated using centered time differences (Δt = 30 min). Figure 20 shows the various components of the vorticity equation for 0600 and 1800 UTC 12 November 1986.

At 6 h (0600 UTC 12 November) there were two major areas of negative local change of relative vorticity. One, located south of the surge over eastern Colorado, was in response to the flow becoming more anticyclonic as the lee trough drifted southward, and a second area was behind the leading edge of the surge from Wyoming to Iowa. Both of these negative tendencies were primarily the result of negative absolute vorticity advection. The frictional generation and divergence terms had only weak negative tendencies north of the leading edge of the surge. The negative tendencies induced by the divergence term from eastern Nebraska northward to Minnesota were associated with low-level diffluent flow across the northern plains and not upslope flow. Meanwhile, vortex stretching was enhancing the vorticity of the lee low around the Texas panhandle.

By 18 h (1800 UTC 12 November), as the leading edge of the surge intensified adjacent to the barrier, the negative relative vorticity tendencies increased as a result of both horizontal advection and frictional generation. The divergence term had a weak area of negative values just south of the Texas panhandle, which was caused by upslope and divergent flow behind the leading edge.

Overall, very little negative relative vorticity was generated by vortex column compression associated with upslope flow. Most of the local vorticity changes behind the surge were the result of horizontal advection during the early hours of the surge (6 h) and a combination of advection and frictional generation several hours later (18 h). Therefore, as in the thermodynamic analysis, the topographic Rossby mechanism for this surge did not seem significant.

6. Simulation without the Gulf of Mexico

A separate simulation was completed to determine whether the change in scale of the pressure ridge along the Mexican coast resulted from 1) the transition from the synoptic-scale sloping lower boundary over the southern plains to an abrupt coastal barrier over Mexico or 2) because the warm gulf waters limited the eastward extent of the cold dome.

To reduce the sensible heat fluxes over the Gulf of Mexico, the model gulf was replaced by flat land.

[9] These "friction" components represent both surface drag and momentum mixing from aloft.

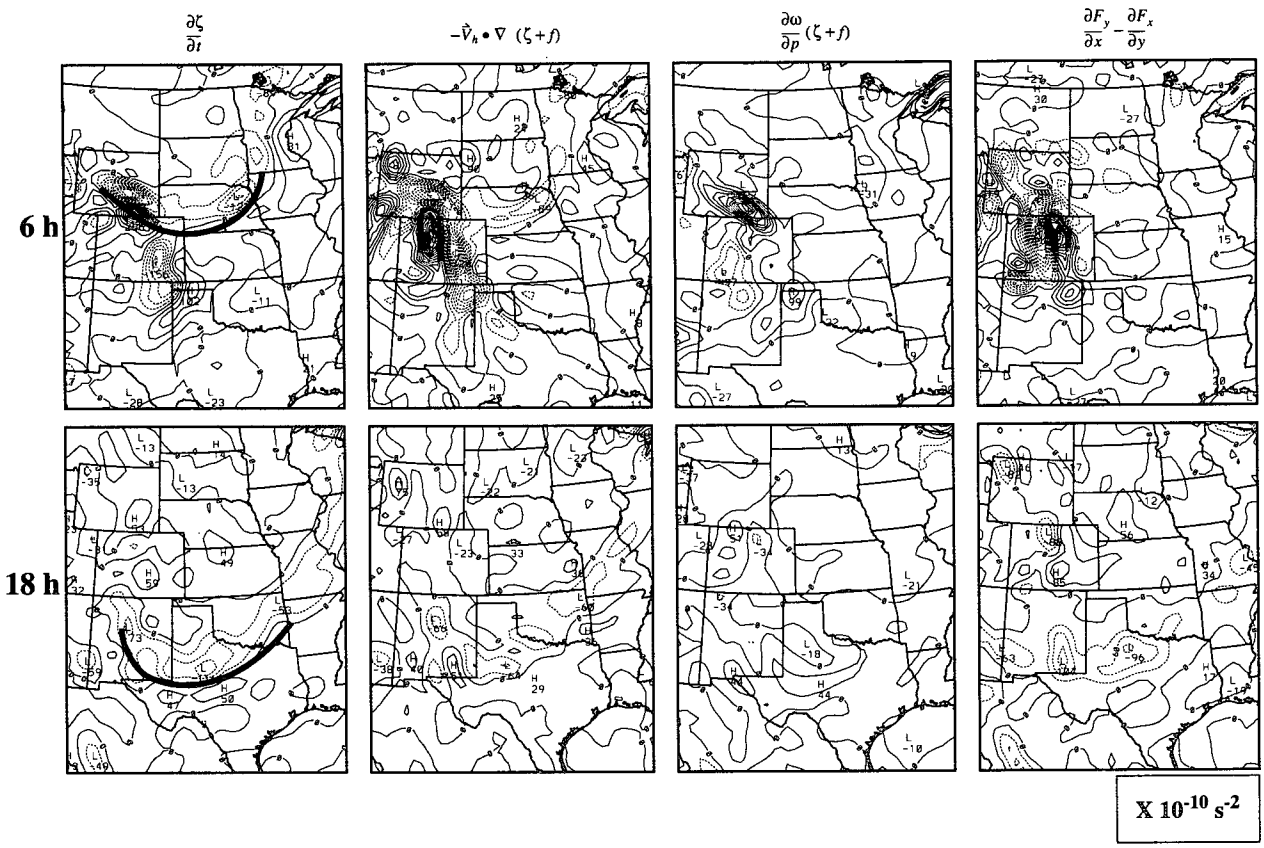

FIG. 20. Diagnosis of the vorticity equation showing local relative vorticity change, horizontal advection of absolute vorticity, divergence, and frictional terms averaged for the lowest five half-sigma levels at 6 and 18 h into the simulations (0600 and 1800 UTC 12 November respectively). The contour interval is 3.0×10^{-9} s^{-2}.

Over the entire model domain, the surface and subsurface temperatures were initialized using the temperature at the lowest half-sigma layer (about 40 m above surface). Figure 21 shows the surface temperature initializations for the original and no-gulf simulations. The no-gulf simulation was run in the same

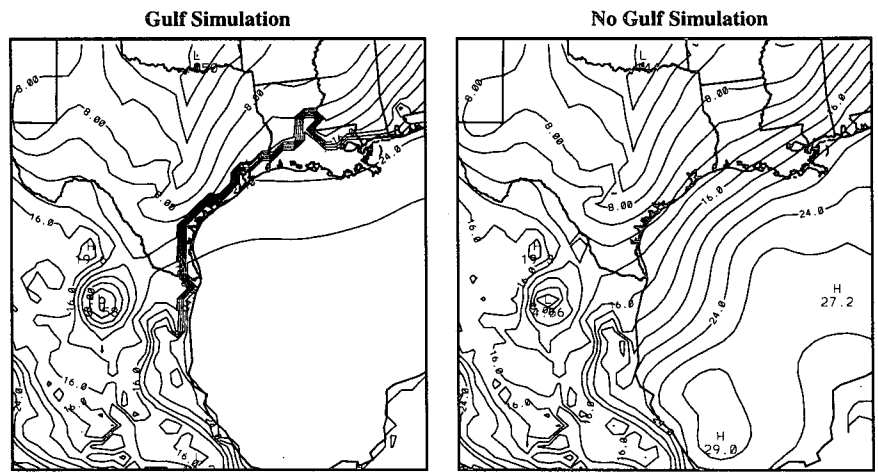

FIG. 21. The model ground temperature initializations at 0000 UTC 12 November 1986 for the simulation with the Gulf of Mexico intact and the no-gulf simulation. The contour interval is 2°C.

manner as the control run, using FDDA for only the first 12 h.[10]

Figure 22 shows the surface structure of the surge at 48 h (0000 UTC 14 November) for the no-gulf simulation. Without the gulf, the cold air advanced southward much farther than in the original simulation (Fig. 16b). (The 16°C isotherm was approximately 450 km further south.) Structurally, a mesoscale pressure ridge still developed along the Mexican coast; however, it was sharper in the control simulation because of the airmass modification by the warm gulf.

Cross sections were taken normal to the pressure ridge at 0000 UTC 14 November in order to compare the vertical structures for the gulf and no-gulf cases (Fig. 23). The line on Fig. 22 shows where the sections were taken. In both cases, a northerly low-level wind maximum of about 20–30 m s^{-1} was located over the lower slopes of the coastal mountains, and the cold dome extended away from the terrain. However, in the no-gulf simulation the cold dome was more intense and extended farther eastward, and the low-level northerly jet was weaker.

Overall, this experiment showed that to first order the scale of the ridging was not an artifact of the warm waters of the gulf limiting the eastward extent of the cold dome; rather, cold-air damming against the coastal barrier was the major contributor to the structure and scale of the pressure ridge. Sensible heating from the gulf decreased the horizontal scale of the damming. This experiment also showed that when the water was replaced by land, the front was able to traverse southward more rapidly and with little frontolysis. The slope of the damming and the cross-barrier pressure gradient were less without the gulf; as a result, the northerly wind maximum was weaker.

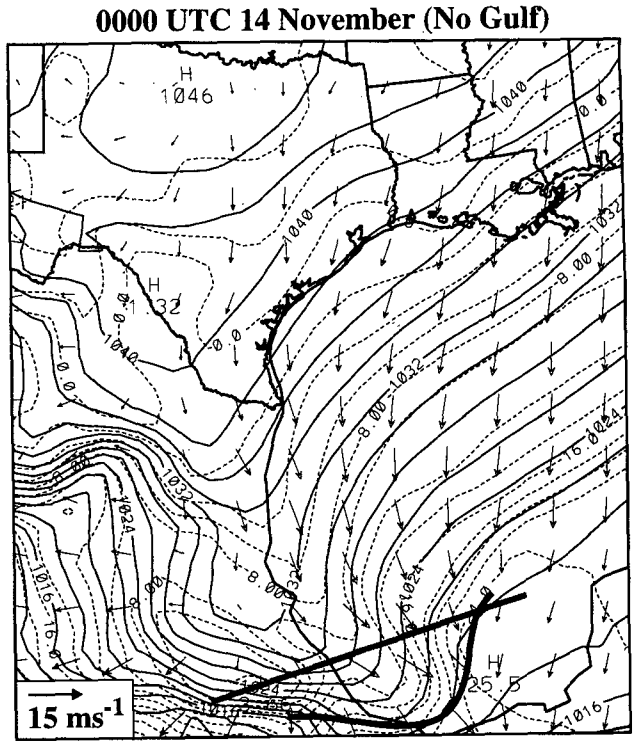

FIG. 22. Model surface analyses for the no-gulf simulation at 0000 UTC 14 November. The contour interval is 2 mb and 2°C for sea level pressure and temperature, respectively, and the wind vectors are in meters per second. The solid line indicates the leading edge of the surge, and the straight line shows the location of the cross section taken for Fig. 23.

7. Discussion of the 12 November 1986 surge

This section examines the applicability of various dynamical explanations for the November 1986 northerly surge event.

a. Ageostrophic downgradient flow and cold-air damming

As noted in section 1, an along-barrier pressure gradient can force ageostrophic downgradient flow. In addition, if an upslope component exists and the Froude number is less than 1, blocking and cold-air damming can result. Northerly surges to the east of the Rockies are often accompanied by Froude numbers less than approximately 0.4 (Tilley 1990), and, in fact, the Froude numbers during the November 1986 event were generally less than about 0.2 (using $U \sim 5$ m s^{-1}, $h_m \sim 1500$ m, $N \sim 2.0 \times 10^{-2}$ s^{-1}).

The evolution of the synoptic-scale along-barrier pressure gradient during the November 1986 case played an important role in the surge evolution. As high pressure spread into the central plains, nearly downgradient northerly flow developed over the region. Lee troughing over the Texas panhandle enhanced the along-barrier pressure gradient and ageostrophic northerlies adjacent to the Rockies. A Coriolis torque acting on this downgradient flow resulted in an upslope component at the forward portion of the surge,[11] which pushed the cold air up the slope. Because of high stability and a sloping lower boundary, the cold air became blocked, resulting in an orographically trapped cold dome, a pressure gradient component parallel to the slope gradient, and terrain-parallel (northerly) flow.

To demonstrate this adjustment process, Fig. 24a shows the flow evolution in a cross section taken normal to the Colorado Rockies (from central Colorado eastward to Illinois). Prior to surge passage at 0600

[10] Because temperatures were not nudged within the PBL, FDDA did not induce low-level warming over the region converted to land.

[11] The Coriolis force is the only force capable of accelerating the flow in the upslope direction; since downgradient acceleration would be toward the surface trough over the Texas panhandle (cf. Fig. 13a).

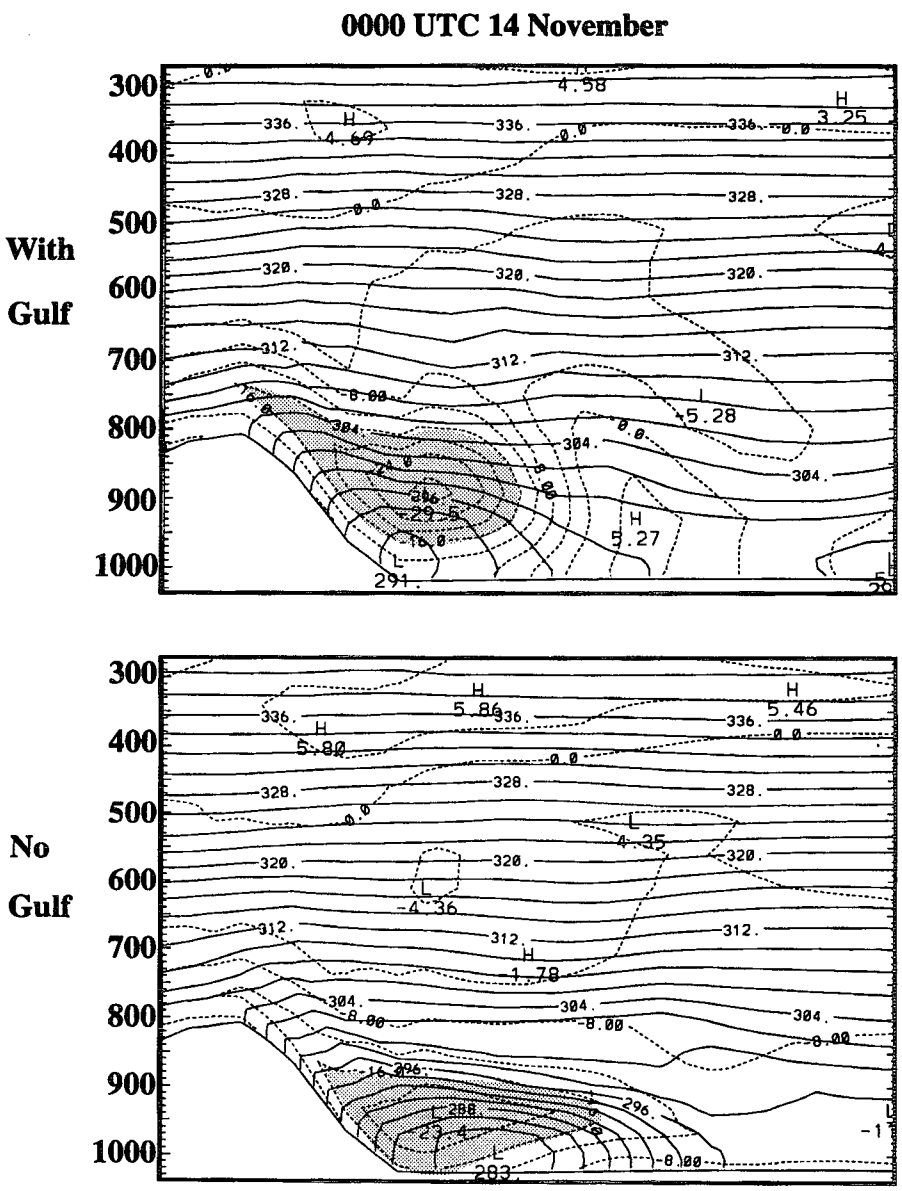

FIG. 23. Model cross sections taken across the line on Fig. 22 for the gulf and no-gulf simulations at 0000 UTC 14 November 1986. The meridional wind component (dashed) and potential temperature (solid) have contour intervals of 4 m s^{-1} and 2 K, respectively. The shading represents northerly wind speeds equal to or greater than 16 m s^{-1}.

UTC 12 November, downslope flow had generated troughing and low stability over the upper portion of the slope, while a preexisting cold stable layer from the previous surge event extended eastward from western Kansas. By 1200 UTC 12 November, about 3 h after the surge entered the cross section, a strong upslope component was present over eastern Colorado and western Kansas, and the isentropes were beginning to tilt in response to the cold air being advected up the barrier. By 1800 UTC 12 November, cold-air damming and northerlies were firmly established over the sloping terrain and the upslope component had lessened. Figure 24b shows an hourly trace of upslope and terrain-parallel flow at the surface (negative u and v components, respectively) for point A along these cross sections from 0600 UTC to 2300 UTC 12 November.[12] Two hours after the passage of the leading edge of the surge

[12] The data used in Fig. 24 originated solely from the simulation without FDDA in order to obtain a continuous wind trace through the period.

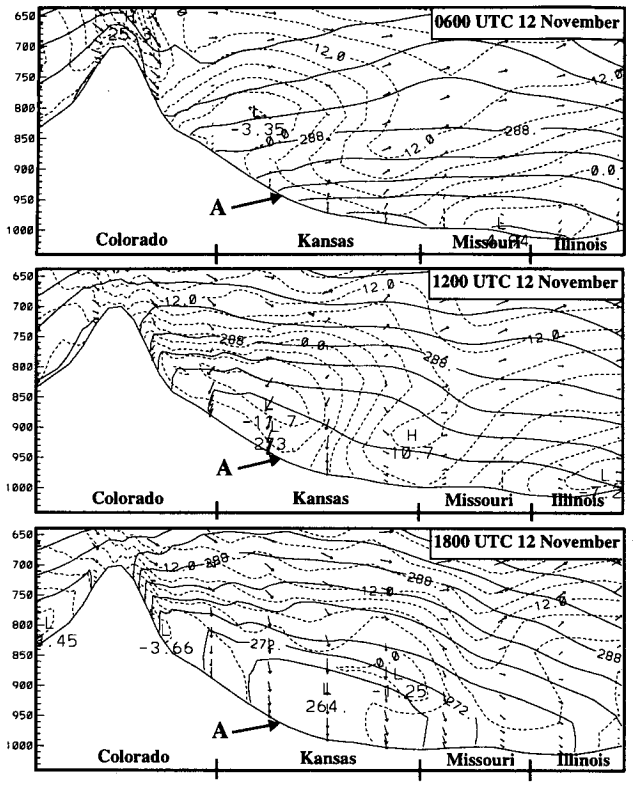

FIG. 24. (a) Model cross sections for 0600, 1200, and 1800 UTC 12 November 1986 showing wind vectors (m s^{-1}), the zonal component of the wind (dashed) contoured every 3 m s^{-1}, and the potential temperature (solid) contoured every 4 K. (b) Surface wind traces normal (u) and parallel (v) to the terrain for point A at 0600 to 2300 UTC 12 November.

at point A (about 1100 UTC 12 November), both components reached their peak. Subsequently, as the upslope flow became blocked and damming occurred, the upslope flow weakened rapidly (from 1200 to 1600 UTC 12 November), while the northerly low-level jet continued for the remainder of the period with far less attenuation. This process was apparent along the entire length of the Rockies as the surge moved southward. Tilley (1990) also noted that a maximum in upslope flow occurs at the forward portion of surges to the east of the Rocky Mountains.

The structural evolution of this cold surge had many characteristics similar to cold-air damming along the Appalachians. As with Appalachian damming, the establishment of an along-barrier pressure gradient led to an enhancement of the northerlies to the east of the barrier, and an upslope component at the leading edge of the surge helped move the cold air up the slope. Bell and Bosart (1988) noted that cold advection accounts for most of the total cooling during Appalachian damming, with adiabatic upslope cooling accounting for only approximately 30%. Similarly, cold advection dominated over adiabatic cooling for the November 1986 surge. For both the Appalachian damming and the 1986 surge, once the upslope flow became blocked, a shallow cold dome, a surface pressure ridge, and a northerly low-level jet developed to the east of the barrier (see cross sections on Fig. 18). The low-level jet remained nearly stationary for several hours within the sloping isentropes, above the location where the terrain slope steepened.

Examining force balances, Bell and Bosart (1988) noted that for Appalachian damming the low-level northerly jet above the surface was in approximate geostrophic balance between the Coriolis force and the pressure gradient force caused by mass accumulation next to the mountains. Near the surface, friction also has a significant component in the cross-barrier direction because of strong vertical momentum mixing (Bell and Bosart 1988). In the along-barrier direction the balance is primarily between the pressure gradient force and friction.

The magnitude of the various terms of the momentum equation were evaluated at 0000 UTC 13 November to determine the force balances for the 1986 surge event (Fig. 25). The vertical advection terms were small and therefore neglected, and the frictional term was calculated as a residual, as in the previous section. As with Appalachian damming in its mature stage, the Lagrangian accelerations at the surface (cf. Fig. 25a) across the southern plains at this time were small, and the mountain-normal pressure gradient induced by the cold dome balanced both the Coriolis force and a component of friction associated with the strong northerly flow. The along-barrier pressure gradient was mostly balanced by frictional processes. However, unlike Appalachian damming, strong ageostrophy and downgradient flow existed far away from the barrier as the cold air spread outward from the anticyclone. At 950 mb, for a line across this cold dome (see line on Fig. 25a), various terms of the momentum equation were calculated both normal and parallel to the mean slope of the terrain (Figs. 25b,c). Normal to the slope, there was approximate geostrophic balance, with the pressure

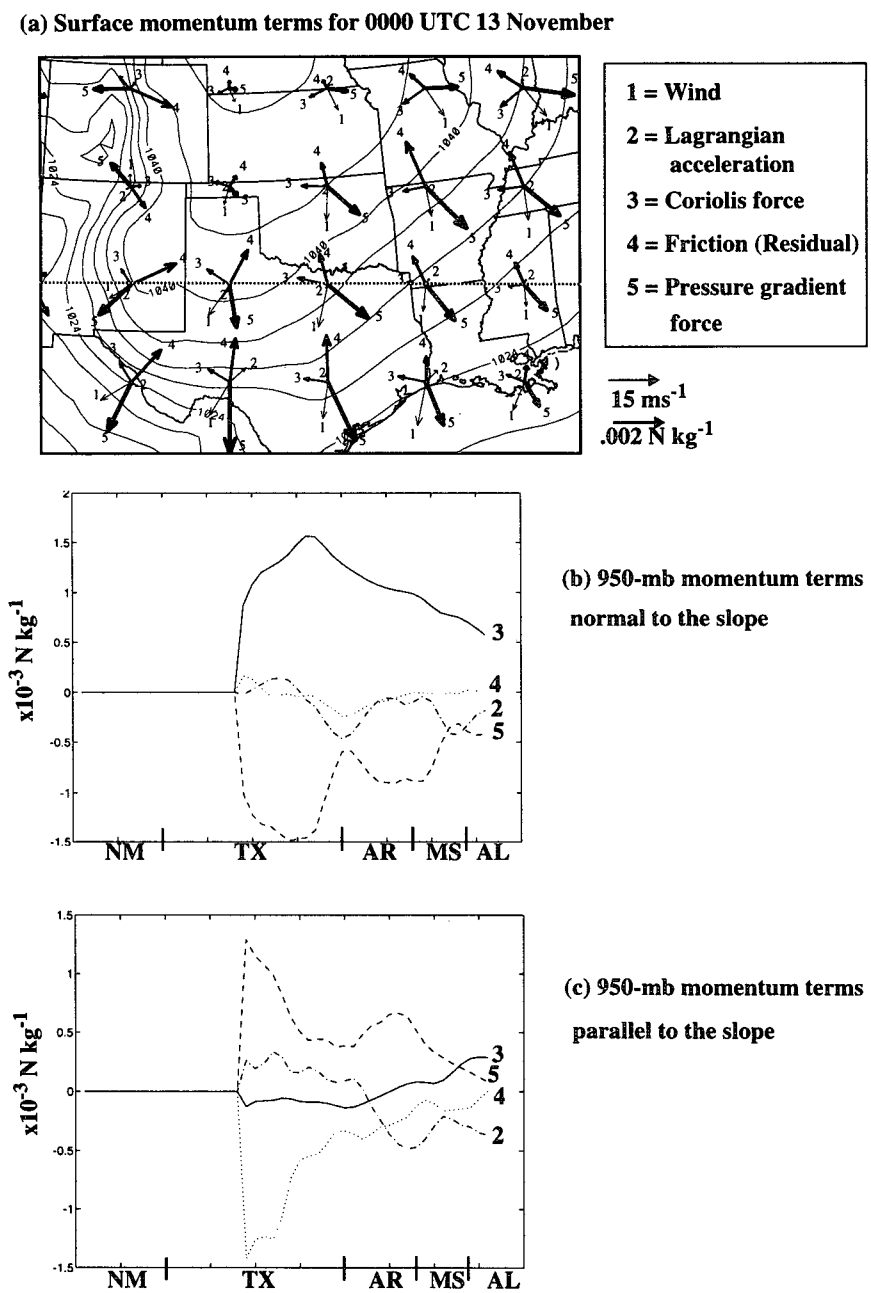

FIG. 25. (a) Surface momentum terms and sea level pressure contoured every 4 mb for 0000 UTC 13 November 1986. The corresponding terms in the momentum equation are defined and numbered above. The 950-mb momentum terms (b) normal and (c) parallel to the slope, respectively, for the line shown in (a).

gradient term balancing the Coriolis force over the eastern half of Texas. In contrast, friction (residual) approximately balanced the pressure gradient force in the terrain-parallel direction. The force balances changed from Louisiana eastward, as the residual (friction) decreased with the lighter winds and the acceleration became more significant around the leading edge of the surge.

Using data from the no-gulf simulation,[13] Fig. 26a shows the 950-mb momentum terms at 1800 UTC 13

[13] The dataset from the no-gulf simulation was used in order to obtain a clearer understanding of the topographic effects without the influences of the strong coastal baroclinic zone and rapid changes in surface drag induced by the land–water transition.

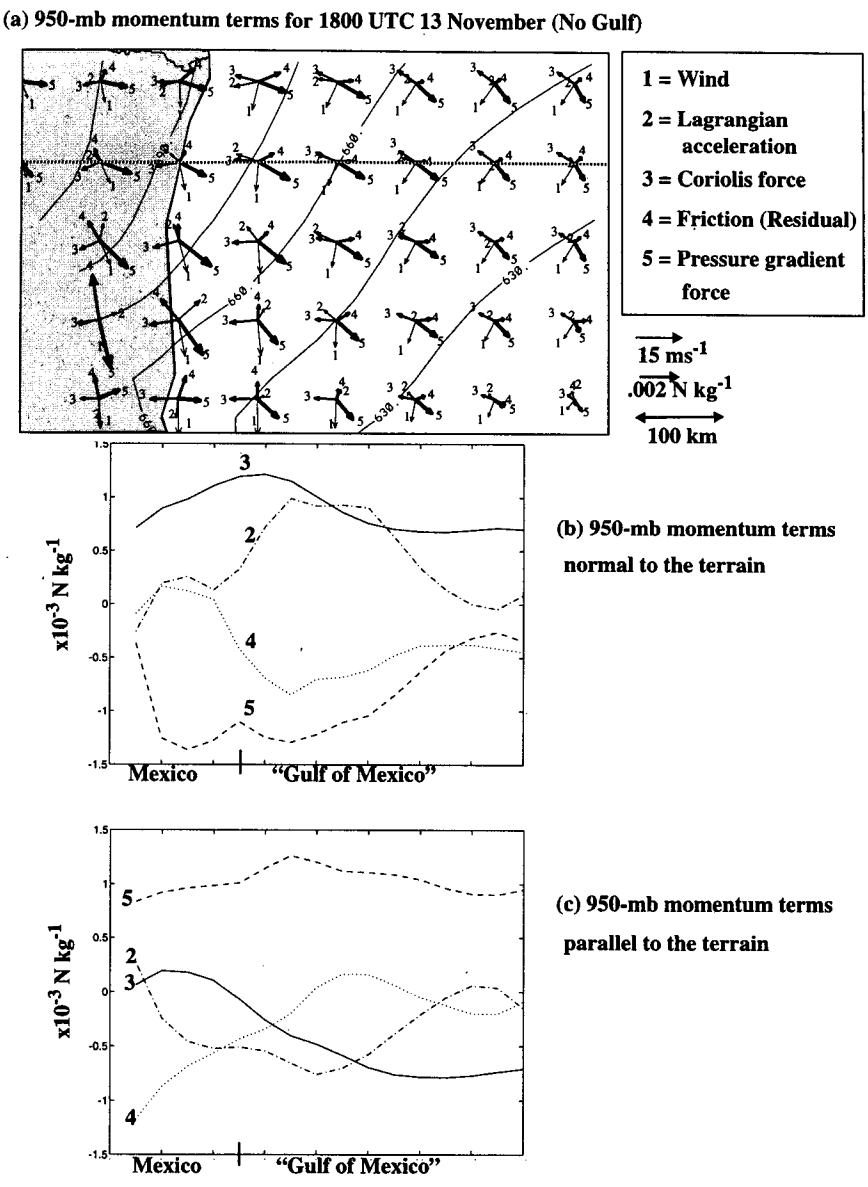

FIG. 26. (a) The 950-mb momentum terms and geopotential heights contoured every 15 m eastward from the Mexican coast (shaded) for 1800 UTC 13 November 1986. The corresponding terms in the momentum equation are defined and numbered above. The 950-mb momentum terms (b) normal and (c) parallel to the slope, respectively, for the line shown in (a).

November when the surge extended along the Mexican coast. Several hundred kilometers to the east of the Mexican coast, the winds were approximately geostrophic. Approaching the coast from the east, the flow became more antitriptic in the terrain-parallel direction as the residual term increased (some of the Lagrangian accelerations were large in response to the curvature in the flow), while the flow was nearly geostrophic in the terrain-normal direction as a result of the damming. Figures 26b,c show explicitly the components of the various terms of the momentum equation for both normal and parallel to the coastal terrain along the line shown on Fig. 26a. Over the coastal areas, the pressure gradient term approximately balanced the Coriolis force in the terrain-normal direction, and the residual (friction) primarily balanced the along-barrier pressure gradient. Farther to the east, the residuals decreased and the flow became more geostrophic.

Overland (1984) noted that when the along-barrier Rossby number V/fl (where V is the along-barrier wind and l is the length is the cross-barrier direction) is about 1 or greater, and l is much less than the along-barrier scale L, the influence of topography should extend about a Rossby radius away from the topography.

This scaling fits well for the cold dome that occurred along the Mexican coast where the Rossby number was approximately 1 ($V \sim 10$–20 m s^{-1}, $f \sim 6.16 \times 10^{-5}$ s^{-1}, and $l \sim 350$ km), and the cross-barrier scale l was much less than L ($\sim$1000 km), and the Rossby radius, $l_R = Nh_m/f \sim 400$ km (where $h_m \sim 1500$ m, $f \sim 6.16 \times 10^{-5}$ s^{-1}, and $N \sim 1.7 \times 10^{-2}$ s^{-1}), was close to the offshore length scale of the surface pressure ridging (and the terrain-parallel flow) shown on Fig. 15. As noted earlier, the no-gulf simulation confirms that the width scale was not primarily an artifact of the warm waters of the gulf limiting the size of the cold dome but rather represents the scale of the damming.

The large width of the cold dome across the southern plains ($l \sim 750$–1000 km) would appear too large for damming dynamics because 1) the Rossby number is much less than one, thus implying quasigeostrophic dynamics, and 2) the width of the cold dome is much larger than the calculated Rossby radius of $\sim$475 km (where $h_m = 2000$ m, $f \sim 8.4 \times 10^{-5}$ s^{-1}, and $N \sim 2.0 \times 10^{-2}$ s^{-1}). However, with the velocities and stabilities observed during the surge ($U \sim 5$ m s^{-1} and $N \sim 2.0 \times 10^{-2}$ s^{-1}), the height of the topography needed only to be $\sim$250 m in order have blocked flow (Froude number less than 1). Given the average slope of the southern plains (1/500), blocking would thus occur within about 100–200 km for any westbound air parcel along the slope. As a result, large-scale damming could have occurred over the sloping Great Plains. Therefore, although a simple scale analysis using the complete width of the cold dome would favor quasigeostrophy, embedded within this large-scale cold dome was smaller-scale damming in which a geostrophic balance existed normal to the barrier, while an antitriptic balance was present in the terrain-parallel direction.

b. *Kelvin waves*

Tilley (1990) suggested that when upslope flow at the leading edge of the surge is blocked around the Colorado Front Range, Kelvin waves are generated that propagate southward along the barrier. In the November 1986 case, the low-level winds over the sloping Great Plains were generally ageostrophic and parallel to the terrain as with Kelvin waves. However, these ageostrophic northerlies developed in situ over the sloping terrain between 0600 and 1200 UTC 12 November as a result of the onset of an along-barrier pressure gradient rather from than a Kelvin wave (cf. Fig. 17). Terrain-parallel flow was maintained by the upslope damming mechanism noted above.

Between 1200 and 2100 UTC 12 November, the surge moved continuously southward across western Texas and its speed was calculated by following the leading edge of the strong northerlies and associated baroclinic zone on horizontal charts and cross sections. The surge moved approximately 15 m s^{-1}, which is less than a calculated Kelvin wave speed ($\sim$23 m s^{-1}, where $\Delta\theta \sim 15$ K, $\theta \sim 280$ K, and $H \sim 1000$ m) and is consistent with advection dominating. The leading edge of the surge did not move faster adjacent to the steep terrain than over level terrain to the east because of the strong ageostrophic flow over both areas. Overall, as the surge moved southward, it was highly advective (as noted by the movement of the cross-section isentropes in Fig. 17 and the dominance of temperature and vorticity advections in the diagnostics) and therefore did not seem "wavelike."

c. *Topographically trapped density currents*

Baines (1980) noted that trapped density currents are associated with rapid wind shifts, wind accelerations, temperature drops, and an e-folding current width close to the Rossby radius of deformation. The leading edge of the November 1986 northerly surge lacked some essential density current characteristics. First, the surge did not propagate southward as a uniform feature between 0600 and 1200 UTC 12 November. Instead, after the along-barrier pressure gradient was established, the leading edge of the surge became reestablished along a weakening surface trough across the Texas panhandle. Second, the temperature transitions were generally not as intense as those associated with gravity currents. For example, as the surge developed across the Texas panhandle around 1200 UTC 12 November, the observed temperature gradient behind the leading edge was only about 3°C (100 km)$^{-1}$ (see the surface analysis on Fig. 6). Frontogenesis tightened the temperature gradients closer to those expected from a gravity current as the surge moved southward over western Texas by 1800 UTC 12 November. However, the strong northerlies existed well in advance of the sharp temperature drops (cf. Fig. 17). In contrast, Sanders (1955) describes the southward movement of an intense cold front through Texas that had characteristics more similar to a gravity current. However, his case was more synoptically forced (stronger west-southwesterly flow at low levels), which led to intense frontogenesis near the surface and, therefore, tighter wind and temperature transitions.

d. *Topographic Rossby and shelf waves*

Because of the sloping surface of the Great Plains, several investigators (Hsu and Wallace 1985; Hsu 1987; Tilley 1990) have suggested that some southward-moving cold surges have properties similar to larger-scale trapped waves such as topographically trapped Rossby waves or shelf waves. For both of these features the upslope motions at the leading section of the surge leads to vortex compression and adiabatic cooling, both of which help extend the anticyclonic tendencies to the south.

Diagnostics were completed for the November 1986 event using the vorticity and thermodynamic energy equations to gain an understanding of the physical processes that moved the surge southward (Figs. 19 and 20). It was shown that both adiabatic cooling and neg-

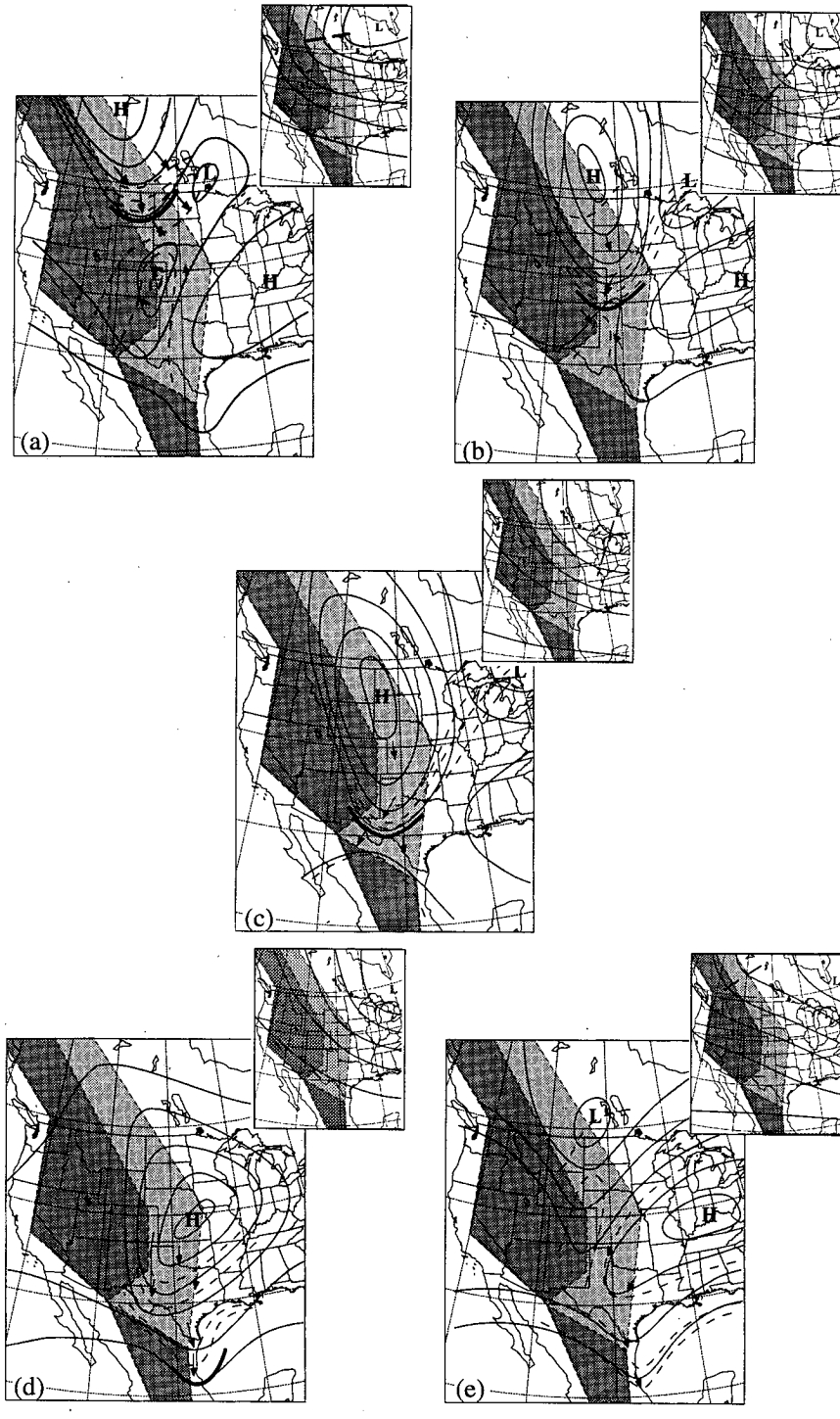

FIG. 27. A conceptual model of the structural evolution of a northerly surge showing 500-mb heights (the axis of the short-wave trough is dashed) as well as sea level pressure, temperature, and winds for the surface. The dark gray represents the Rocky Mountains, and the lighter gray shows the sloping Great Plains.

ative vorticity generation by upslope motions were generally much smaller than the thermal and absolute vorticity advections. Therefore, these surges were not bounded to the terrain primarily because of topographically trapped Rossby or shelf wave dynamics. The lee trough, which aided the southward movement of the surge by enhancing the along-barrier pressure gradient, superficially might seem analogous to the topographic Rossby wave because it appeared to propagate southward from eastern Colorado to New Mexico and its generation and maintenance was primarily due to lee side adiabatic warming. However, the trough was forced by the cross-barrier synoptic-scale flow, which was veering with time, rather than being a freely propagating wave.

8. Summary of the 28–30 January 1993 surge event

A weaker surge event (28–30 January 1993) was also analyzed in order to examine the generality of the results derived from the November 1986 surge. In this case, surface troughing also developed to the south of the surge; however, it was the result of a weak closed low/trough aloft propagating over the southern plains. As in the stronger November 1986 case, this surface troughing resulted in the enhancement of the ageostrophic northerlies near the leading edge of the surge. An upslope component at the forward edge of the surge led to the same damming evolution discussed in this paper. A dynamical analysis conducted on this weaker case showed that the surge was highly advective, both in temperature and vorticity, and, therefore, had dynamics similar to damming and not Kelvin or topographic Rossby/shelf waves.

9. A conceptual model of a northerly cold surge east of the Rockies

Based on the two case studies, which used both model and actual data, and the composite surge event, a conceptual model of the evolution of a northerly surge is presented in Fig. 27. During the early stages of the surge event (Fig. 27a), a 500-mb long-wave ridge is present along the West Coast, and a long-wave trough is situated over the eastern half of the United States. An anticyclone over southwestern Canada is behind a short-wave trough moving southeastward through the ridge. Strong cross barrier flow[14] to the south of the short-wave trough produces a mesoscale lee trough and low-level warm anomaly east of the Rockies (over eastern Colorado and New Mexico). Weak northerlies and some baroclinity extend northward from this trough. However, the more intense northerlies and temperature gradient exist across Montana and North Dakota, which are immediately behind the leading edge of the surge. Weak pressure ridging is present over the southern states and Mexican coast from a previous surge or cold outbreak.

During the next several hours (Fig. 27b), as the low-level ridging moves southward over the northern plains and the lee trough becomes situated over western Texas, the along-barrier pressure gradient and ageostrophic northerlies are enhanced to the east of the Colorado Rockies. The Coriolis force acting on this downgradient flow results in an upslope component near the leading edge of the surge, which advects cold air up the barrier, resulting in damming. The baroclinic zones associated with the cold air moving southward from the northern plains and the lee trough merge, with the leading edge of the surge now along the northern portion of the lee trough. Weak northerlies or downslope northwesterlies exist ahead of the leading edge of the surge. In addition, significant ageostrophic flow exists well to the east of the barrier as cold air spreads outward from the anticyclone.

As the 500-mb short-wave trough axis shifts east of the Rocky Mountains and the flow becomes more northwesterly across the barrier, the upper-level pattern becomes less favorable for lee troughing (Fig. 27c). As a result of this change and cold air reaching the trough, the presurge trough weakens or is lost. The along-barrier pressure gradients continue to favor enhanced northerlies to the east of the Rockies, and an upslope component still exists near the leading edge of the surge; the previous upslope flow to the north over Nebraska and Kansas has become more terrain parallel as a result of the damming.

Approximately two days after the initiation of the event, a large-scale pressure ridge is established across the southern plains (Fig. 27d). The pressure ridging over Texas intensifies the along-barrier pressure gradient to the south. As a result, ageostrophic northerlies, cold advection, and upslope flow leads to damming along the Mexican coast, in which a pressure ridge develops. The scale of the pressure ridging is much smaller than over the plains because a large-scale slope does not exist over eastern Mexico.

During the next day, lee troughing or cyclogenesis often occurs along the eastern slopes of the Rockies as a result of strong cross-barrier flow associated with the approach of another shortwave trough (Fig. 27e). The pressure ridging over the southern plains begins to decay as the winds within the pressure ridge become southerly. The main anticyclone drifts eastward toward the Ohio Valley with the upper-level short-wave trough, while surface ridging is still strong along the eastern Mexican coast. Thus, during this later period, the thermal and pressure fields develop a two-lobe structure.

Acknowledgments. This research was funded by the National Science Foundation under Grant ATM-9111011. Use of the MM4 was made possible by the Microscale and Mesoscale Meteorological Division of the National Center for Atmospheric Research (NCAR). The mesoscale model was run at the Scien-

[14] The January 1993 evolution of the surge involving the generation of the surface trough by the cutoff low aloft was ignored in this conceptualization given the infrequent occurrence of this scenario.

tific Computing Division of NCAR. We acknowledge Jim Steenburgh's assistance in running the MM4 and for his review of the paper, and Jonathan Martin, Jon Locatelli, James Overland, and Mike Wallace, whose comments greatly improved this manuscript. We also wish to thank Ernie Recker for acquiring the observational data, Mark Albright's suggestions in improving the surface analyses, and Kay Dewar for helping prepare some of the figures.

REFERENCES

Anh, N. N., and A. E. Gill, 1981: Generation of coastal lows by synoptic-scale waves. *Quart. J. Roy. Meteor. Soc.*, **107,** 521–530.

Anthes, R. A., and T. T. Warner, 1978: Development of hydrodynamic models suitable for air pollution and other mesometeorological studies. *Mon. Wea. Rev.*, **106,** 1045–1078.

——, E. Y. Hsie, and Y. H. Kuo, 1987: Description of the Penn State/NCAR mesoscale model version 4 (MM4). NCAR Tech. Note NCAR/TN-282+STR, 66 pp.

Baines, P. G., 1980: The dynamics of the southerly buster. *Aust. Meteor. Mag.*, **28,** 175–200.

Baker, D. G., 1970: A study of high pressure ridges to the east of the Appalachian Mountains. Ph.D. thesis, Massachusetts Institute of Technology, 127 pp.

Bannon, P. R., 1981: Synoptic scale forcing of coastal lows; forced double Kelvin waves in the atmosphere. *Quart. J. Roy. Meteor. Soc.*, **107,** 812–829.

Bell, G. D., and L. F. Bosart, 1988: Appalachian cold-air damming. *Mon. Wea. Rev.*, **116,** 137–161.

Benjamin, S. G., 1983: Some effects of surface heating and topography on the regional severe storm environment. Ph.D. dissertation, The Pennsylvania State University, 265 pp.

Bluestein, H. B., 1993: *Synoptic–Dynamic Meteorology in Midlatitudes; Observations and Theory of Weather Systems.* Vol. 2, Oxford University Press, 594 pp.

Colquhoun, J. R., D. J. Shepard, C. E. Coulman, R. K. Smith, and K. McInnen, 1985: The southerly buster of southeastern Australia: An orographically forced cold front. *Mon. Wea. Rev.*, **113,** 2090–2107.

Coulman, C. E., J. R. Colquhoun, R. K. Smith, and K. McInnes, 1985: Orographically-forced cold fronts-mean structure and motion. *Bound.-Layer Meteor.*, **32,** 57–83.

Dorman, C. E., 1985: Evidence of Kelvin waves in California's marine layer and related eddy generation. *Mon. Wea. Rev.*, **113,** 827–839.

Dunn, L., 1987: Cold-air damming by the Front Range of the Colorado Rockies and its relationship to locally heavy snows. *Wea. Forecasting,* **2,** 177–189.

Forbes, G. S., R. A. Anthes, and D. W. Thomson, 1987: Synoptic and mesoscale aspects of an Appalachian ice storm associated with cold air damming. *Mon. Wea. Rev.*, **115,** 564–591.

Gill, A. E., 1977: Coastally trapped waves in the atmosphere. *Quart. J. Roy. Meteor. Soc.*, **103,** 431–440.

——, 1982: *Atmospheric–Ocean Dynamics.* International Geophysics Series, Vol. 30, Academic Press, 662 pp.

Grell, G., Y. H. Kuo, and R. Pasch, 1988: Semi-prognostic test of three cumulus parameterization schemes for mid-latitude convective systems. *Proc. Eighth Conf. on Numerical Weather Prediction,* Baltimore, MD, Amer. Meteor. Soc., 363–370.

Hoinka, K. P., and H. Volkert, 1992: Fronts and the alps: Findings from the front experiment 1987. *Meteor. Atmos. Phys.*, **48,** 51–75.

Holland, G. J., and L. M. Leslie, 1986: Ducted coastal ridging over southeast Australia. *Quart. J. Roy. Meteor. Soc.*, **112,** 731–748.

Hsie, E.-Y., R. A. Anthes, and D. Keyser, 1984: Numerical simulation of frontogenesis in a moist atmosphere. *J. Atmos. Sci.*, **41,** 2581–2594.

Hsu, H. H., 1987: Propagation of low-level circulation features in the vicinity of mountain ranges. *Mon. Wea. Rev.*, **115,** 1864–1891.

——, and J. M. Wallace, 1985: Vertical structure of wintertime teleconnection patterns. *J. Atmos. Sci.*, **42,** 1693–1710.

Kieser, E. A., 1987: A statistical and structural analysis of Appalachian cold-air damming of various intensities. M.S. thesis, Department of Meteorology, The Pennsylvania State University, University Park, PA, 202 pp.

Lackmann, G. M., and J. E. Overland, 1989: Atmospheric structure and momentum balance during a gap-wind event in the Shelikof Strait, Alaska. *Mon. Wea. Rev.*, **117,** 1817–1833.

Leathers, D. L., 1986: Edge wave characteristics of East Asian cold surges. M.S. thesis, Department of Meteorology, The Pennsylvania State University, University Park, PA, 108 pp.

Mass, C. F., and M. D. Albright, 1985: A severe windstorm in the lee of the Cascade Mountains of Washington state. *Mon. Wea. Rev.*, **113,** 1261–1281.

——, and ——, 1987: Coastal southerlies and alongshore surges of the west coast of North America: Evidence of mesoscale topographically trapped response to synoptic forcing. *Mon. Wea. Rev.*, **115,** 1707–1738.

——, H. J. Edmon, H. J. Friedman, N. R. Cheney, and E. E. Recker, 1987: The use of compact discs for the storage of large meteorological and oceanographic data sets. *Bull. Amer. Meteor. Soc.*, **68,** 1556–1558.

McBride, J. L., and K. L. McInnes, 1993: Australian southerly busters. Part II: The dynamical structure of the orographically modified front. *Mon. Wea. Rev.*, **121,** 1921–1935.

Nakamura, H., and T. Murakami, 1983: Orographic effects on cold surges and lee-side cyclogenesis as revealed by a numerical experiment, Part II, transient aspects. *J. Meteor. Soc. Japan,* **61,** 547–567.

Newton, C. W., 1956: Mechanisms of circulation change during a lee cyclogenesis event. *J. Meteor.*, **13,** 528–539.

Overland, J. E., 1984: Scale analysis of marine winds in straits and along mountainous coasts. *Mon. Wea. Rev.*, **112,** 2532–2536.

——, and N. Bond, 1993: The influence of coastal orography: The Yakutat storm. *Mon. Wea. Rev.*, **121,** 1388–1397.

Panofsky, H. A., and G. W. Brier, 1968: *Some Applications of Statistics to Meteorology.* The Pennsylvania State University, 224 pp.

Pedlosky, J., 1987: *Geophysical Fluid Dynamics.* Springer-Verlag, 710 pp.

Reason, C. J., M. J. Jury, 1990: On the generation and propagation of the southern African coastal low. *Quart. J. Roy. Meteor. Soc.*, **116,** 1133–1151.

——, and D. G. Steyn, 1992: The dynamics of coastally trapped mesoscale ridges in the lower atmosphere. *J. Atmos. Sci.*, **49,** 1677–1692.

Rhines, P. B., 1970: Edge-, bottom-, and Rossby waves in a rotating stratified fluid. *Geophys. Fluid Dyn.*, **1,** 273–302.

Sanders, F., 1955: An investigation of the structure and dynamics of an intense surface frontal zone. *J. Meteor.*, **12,** 542–552.

Stauffer, D. R., and N. L. Seaman, 1990: Use of four-dimensional data assimilation in a limited-area mesoscale model. Part I: Experiments with synoptic scale data. *Mon. Wea. Rev.*, **118,** 1250–1277.

Sumi, A., 1985: A study on cold surges around the Tibetan Plateau by using numerical models. *J. Meteor. Soc. Japan,* **63,** 377–395.

——, and T. Toyota, 1988: Observational study on air-flow around the Tibetan Plateau. *J. Meteor. Soc. Japan,* **66,** 113–123.

Tilley, J. S., 1990: On the application of edge wave theory to terrain-bounded cold surges: A numerical study. Ph.D thesis, The Pennsylvania State University, University Park, PA, and NCAR, Boulder, CO., 353 pp.

Webster, P. J., and J. M. Fritsch, 1985: Edge waves: Ubiquitous, multiscale atmospheric phenomena. *Extended Abstracts, Second Conf. on Mesoscale Processes,* University Park, PA, Amer. Meteor. Soc., 72 pp.

Wilson, K. J., and H. Stern, 1985: The Australian summertime cool change. Part I: Synoptic and subsynoptic scale aspects. *Mon. Wea. Rev.*, **113,** 177–201.

Zhang, D., and R. A. Anthes, 1982: A high-resolution model of the planetary boundary layer sensitivity test and comparisons with SESAME-79 data. *J. Appl. Meteor.*, **21,** 1594–1609.